MASTERARBEIT

Titel der Masterarbeit

„Co-application of bone morphogenetic protein 2 and osteogenic medium enhances osteogenic differentiation of mesenchymal stem cells in 2D and 3D culture"

verfasst von

Alice Zimmermann, BSc

angestrebter akademischer Grad

Master of Science (MSc)

Wien, August 2013

Danksagung

Ich möchte mich bei allen Personen herzlich bedanken, die mich bei meiner Masterarbeit tatkräftig unterstützt haben und mir stets zur Seite gestanden sind.

Ganz besonderer Dank gilt Univ. Prof. Dr. Heinz Redl, Leiter des Ludwig Boltzmann Institutes für experimentelle und klinische Traumatologie, ohne den diese Arbeit nie zu Stande gekommen wäre!

Außerdem möchte ich mich bei Dr. Susi Wolbank und Dr. Georg Feichtinger bedanken, die mich mit ihrem Fachwissen tatkräftig unterstützt haben, sowie Dr. Tatjana Morton die mir stets mit Rat und Tat zur Steite stand.

Besonderer Dank auch an meine Kollegen/innen Mag. Ara Hacobian, Mag. Deniz Öztürk, Mag. Asmita Banerjee, Arife Sener, Mag. Veronika Hruschka, David Hercher und auch an diejenigen, die mir bei Problemstellungen geholfen haben.

Weiters möchte ich mich bei Univ. Prof. Dr. Johannes Nimpf bedanken, der mir durch seine Betreuung von Seiten der Universität es ermöglich hat diese Masterarbeit durchzuführen.

Viel Dank gebührt auch meiner Familie und meinen Freunden, die mir stets zur Seite standen und durch deren gezielte Ablenkung konnte ich wieder neue Kraft schöpfen.

Abstract

Backround: Bone morphogenetic proteins (BMPs) are secreted polypeptides that appear as homo- or heterodimer and belong to the multifunctional TGF-ß family (growth, proliferation, differentiation). Their high osteoinductive potential, particularly of BMP2 and BMP7, has been proved to be successful in bone formation *in vitro* and *in vivo*. Due to the fact that a suitable biomaterial can enhance BMPs' bone forming activity by a continuous long-term plasmid release, fibrin, a natural derived biocompatible polymer was used as 3D scaffold for mesenchymal stem cells in this study.

Objectives: The aim of the study was to analyse the differentiation potential of BMPs as recombinant growth factor and as gene therapy approach in 2D and 3D, as well as to examine the suitability of fibrin as osteogenic biomaterial for rat adipose-derived stem cells (rADSCs).

Methods: The growth factor and plasmid-induced osteogenic differentiation (4 weeks) in 2D was verified by a specific calcium staining (Alizarin-Red staining), quantitative RT-PCR for specific osteogenic markers and BMP2 ELISA. The effect of fibrin as biomaterial on differentiation was analysed by quantitative RT-PCR for osteogenic markers and light microscopy.

Results: Expression levels of osteocalcin, alkaline phosphatase and sialophosphoprotein I were up regulated in BMP2/7 transfected cells compared to reporter gene transfected (GFP positive) cells. Further, the presence of an osteoinductive medium was clearly sufficient to induce osteocalcin and sialophoshoprotein in all samples. A BMP2 ELISA confirmed the impact of this medium on osteogenic differentiation. Last, it could be determined in 2D that a BMP2/7 heterodimer has a high osteoinductive potential on rADSCs, which was however not visible in combination with the osteogenic medium or therapeutic protein. These results were verified by alizarin-red staining, a staining that colours mineral deposits red.

In the next step the impact of fibrin clots on osteogenic differentiation of rADSCs in 3D was determined by quantitative RT-PCR.

At mRNA level, rADSCs cultured in an osteogenic medium show an especially high osteocalcin and sialophosphoprotein expression, if they are treated additionally with 300 ng rhBMP2. This observation is consistent with results in 2D, but reaches a remarkably high level of up regulation in 3D. Interestingly, a uniform expression level of collagen type I was detected in all samples. Probably, a definite amount of collagen fibers has already be produced in the fibrin clots for following differentiation and deposition of specific osteogenic proteins.

Zusammenfassung

Einleitung: Knochenmorphogenetische Proteine (bone morphogenetic proteins, BMPs) sind sezernierte Polypeptide, die als Homo- oder Heterodimer vorliegen können und zur multifunktionellen TGF-ß Familie (Wachstum, Proliferation, Differenzierung) gehören. Ihr hohes osteoinduktives Potential, besonders von BMP2 und BMP7, wurde schon oft in diversen Studien *in vitro* und *in vivo* gezeigt. Dieses kann nur in Kombination mit einem geeigneten Biomaterial, welches eine lang anhaltende kontinuierliche Freisetzung ermöglicht, völlig ausgeschöpft werden. Hierfür wurde in meiner Arbeit Fibrin eingesetzt, da es ein natürlich vorkommendes biokompatibles Polymer ist.

Ziele: Das Ziel dieser Studie war es, das Differenzierungspotential von BMPs in 2D und 3D zu untersuchen, sowie die Eignung von Fibrin als osteogenes Biomaterial in Kombination mit mesenchymalen Rattenstammzellen aus Fettgewebe (rat adipose-derived stem cells, rADSCs) zu testen.

Methoden: Die 4-wöchige Wachstumsfaktor- und Plasmid-induzierte osteogene Differenzierung der mesenchymalen Stammzellen wurde in 2D durch eine spezifische Kalzium-Färbung, quantitative RT-PCR und ELISA untersucht. In 3D erfolgte der Nachweis mittels Lichtmikroskopie sowie RT-PCR.

Ergebnisse: Die Expressionen der osteogenen Marker Osteokalzin, alkalische Phosphatase und Sialophosphoprotein I waren in BMP2/7 transfizierten Zellen im Vergleich zu GFP transfizierten Zellen erhöht. Diese Zellen zeigten eindeutig den Einfluss eines osteogenen Mediums auf die Differenzierung, indem dieses eine Osteocalcin- und SPP-Expression in allen Proben herbeiführte. Ein BMP2 ELISA konnte die osteogen stimulierende Wirkung dieses Mediums bestätigen. Zuletzt konnte in 2D nachgewiesen werden, dass ein BMP2/7-Plasmid eine hohe Osteoinduktivität besitzt, jedoch das Differenzierungspotential erheblich eingeschränkt ist, wenn ein osteogenes Medium mit 300 ng rhBMP2 im Einsatz ist. Weiters wurden die gemessenen Werte mit einer Alizarin-Rot Färbung bestätigt, eine Färbung, die vorhandene Kalziumablagerungen in Osteozyten rot einfärbt.

In Folge wurde der Einfluss eines Fibrinklots auf die osteogene Differenzierung von Fettstammzellen in 3D Kultur mit quantitativer RT-PCR untersucht.

Es konnte mittels RT-PCR nachgewiesen werden, dass rADSCs in einem osteogenen Medium eine besonders hohe Expression von Osteokalzin und Sialophosphoprotein haben, wenn sie mit 300 ng rhBMP2 behandelt werden. Diese Beobachtung bekräftigt die Resultate in 2D, wobei in 3D eine vielfache Expression dieser osteogenen Marker gemessen werden konnte. Interessanterweise wurde in allen Fibrinklots eine einheitliche Kollagen Typ I Expression vorgefunden, worauf zu schließen ist, dass wahrscheinlich in allen Proben bereits eine optimale Dichte des Kollagengrundgerüsts (für die Ablagerungen von knochenspezifischen Proteinen) im Rahmen der Osteogenese erreicht wurde.

Table of contents

1 Introduction

Bone tissue is a specialized form of connective tissue with crucial supportive and protective functions in higher vertebrates. Its mineralized extracellular matrix is not only source of inorganic ions in the body (therefore important in calcium homeostasis), but also responsible for the remarkable rigidity and strength of the skeleton, at the same time retaining some kind of elasticity [1]. Furthermore, bone comprises the bone marrow, the source of white and red blood cells [2].

According to recent studies, 700.000 Austrians are affected by osteoporosis, a disease, which highly increases the risk of fractures. Due to the fact that to date four out of ten women and three out of ten men suffer from fractures, which are often caused by osteoporosis, the future costs will charge the health system. Recently, the WHO has published that approximately half of the fracture patient have a reduced bone mass. Therefore cost-effective, easily applicable and successful treatments for bone defects are under development. Additionally risk factors are nowadays discussed like sufficient consumption of vitamin D and calcium for precaution, which also serves as basis medication of osteoporosis [3].

Clinical status in fracture healing

Fracture healing is a complex multistep process dependent on temporal and spatial coordination as well as interaction of cells (hematopoietic, immune cells, osteoblasts and chondroblasts) and factors, regulating cellular regenerative processes [4]. The aim of fracture treatment is to increase union, because 5-10% of all fractures are accompanied by impaired healing [5]. Presently bone grafting is performed in the clinics for fractures that fail full regeneration (atrophied regions, age related, extensive damage) [6], illustrated in figure 1.
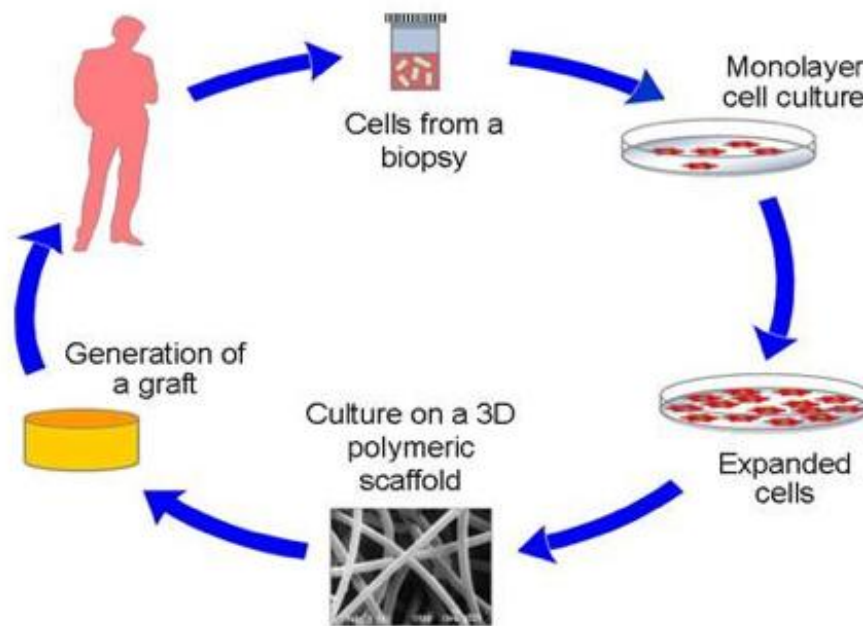
Figure 1: Basic principles of tissue engineering. The idea is to harvest the patient's own material (autologous) which is then placed in a scaffold, which supports formation of bone and integration of the surrounding bone (osteoconductivity) in the defect.

Alternatives for autologous bone grafting are allogenic and xenogenic bone grafting. Furthermore, to minimize invasiveness, injectable systems are under investigation. Due to the fact that loads of implanted cells do not sufficiently engraft *in vivo*, additional osteoinductive factors are an option for bone tissue engineering by inducing differentiation of adjacent non-osteogenic cells to osteoblasts [6]. For this purpose, bone morphogenetic proteins (BMPs), especially BMP2 and BMP7, have explicitly shown their potential as osteoinductive factors in bone formation, particularly in combination with a biomaterial (collagen, hydroxyapatite demineralized bone matrix) [7].

Another solution for this problem can be found in gene therapy. Thereby, it has been shown in several studies that co-transfection of BMP2 and BMP7 has an especially high osteogenic potential and enhances bone formation many fold compared to the application of BMP2 or BMP7 alone [8]. Current research is engaged in finding an appropriate carrier system to enhance the osteoinductive potential of BMPs [9].

1.1 Bone Structure

1.1.1 Types of Bones

Macroscopically, the skeleton is built up of:

- long bones (like the humerus and femur),
- flat bones (like the skull) and
- cuboid bones (like carpals).

Microscopically, bone can be divided into:

- cancellous (spongy, trabecular) and
- compact (cortical) bone [6] (figure 2).

Figure 2: Overview of the structure of a femur: (A) showing the cortical bone outside and the spongy bone inside of the bone, (B-E) depict the tw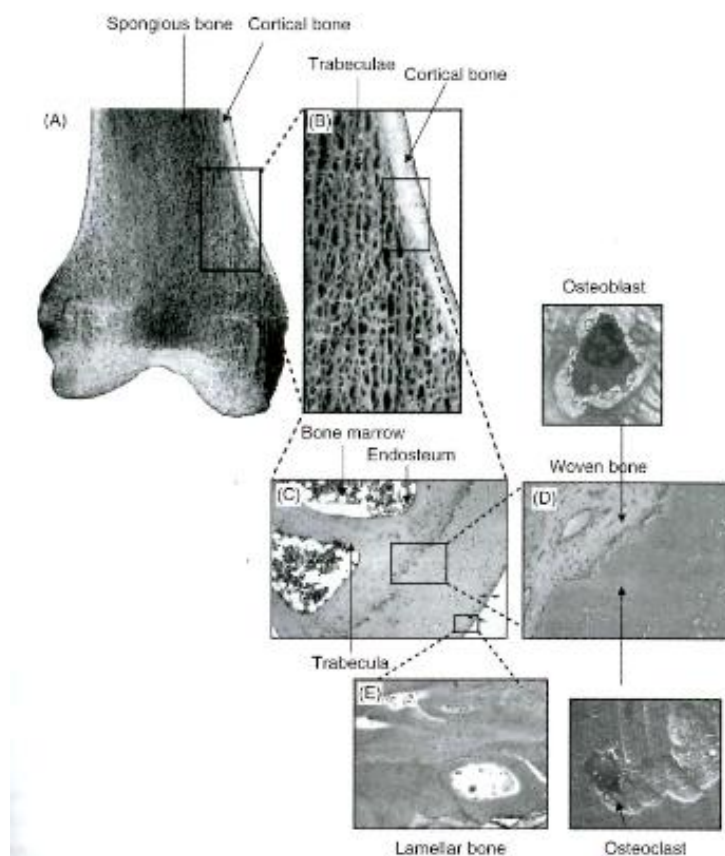o main histological structures in detail: unorganised structure of woven bone, built up of trabeculaes portrayed in (C), (D) interaction of osteoblasts and osteoclasts in localizations of active bone formation and finally finished remodelled lamellar bone is depicted in (E).

1.1.2   Extracellular Matrix (ECM)

Bone consists mainly of collagen type I fibers and hydroxyapatite crystals and to some extent of proteoglycans, glycoproteins and inorganic ions. The chemical composition in weight is: 45% minerals, 30% organic material and 25% water. The combination of collagen and hydroxyapatite crystals makes bone to a highly stable structure, having a high resistance to pressure on the one hand, and to tension on the other hand [10].

Collagens are a family of triple helical proteins playing a role in tissue scaffolding, cell migration, cell adhesion and angiogenesis. Their integrine adhesion sequences like RGD (Arg-Gly-Asp) are involved in integrine ligand binding specificity involved in cellular attachment [11]. Collagen fibrils are organized in a meshwork in woven (spongy) bone, and ordered concentric around the Haver`s canals in lamellar bone, thereby changing it's orientation from one lamellar to the other. Spongy bone is always synthesized when bone tissue has to be produced in a short period of time (embryogenesis, growth plate, fracture repair), but gets naturally remodelled to lamellar bone afterwards [10].

1.1.3   Bone Tissue Cells

Bone tissue contains three different types of cells: osteoblasts, osteoclasts and osteocytes.

Osteoblasts are bone-forming cells with a prominent golgi apparatus and a well developed rough endoplasmic reticulum (rER). Collagen type I and other typical noncollagenous proteins (e.g.: osteocalcin) for bone tissue are synthesized by these cells and are necessary for the following mineralization of the osteoid (ossification).

Osteoclasts are multinucleated bone resorbing cells, which arise from the fusion of uninucleated progenitor cells. Active osteoclasts are lying directly to the mineralized matrix with their ruffled border, a specialization of the plasma membrane. This infolded region contains ATPases, which pump protons into the lacuna to dissolve

the calcium connections. Afterwards, lysosomal enzymes are secreted to destruct the organic matrix. Among them, the cysteine protease cathepsin K is of most importance [reviewed in 2] (figure 3).
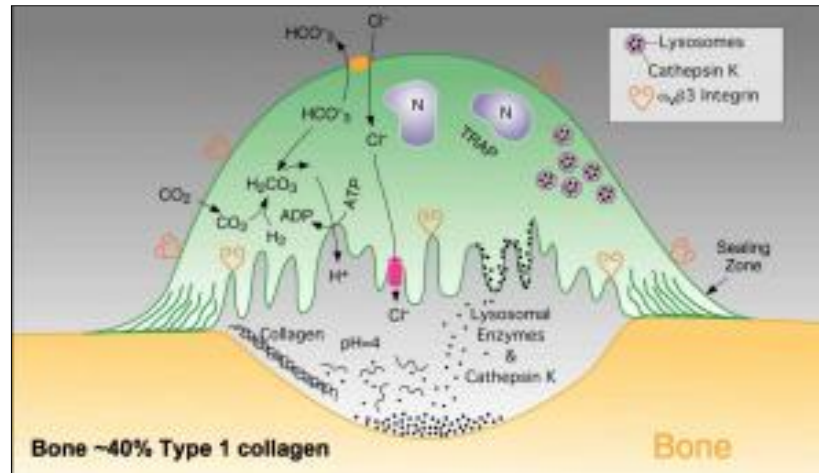
Figure 3: Function of osteoclasts. Active osteoclasts show a typical morphology: sealing zones and a ruffled border. Lysosomal enzymes and H+ are secreted into the howship`s lacune (resorption bay) for bone matrix resorption [2].

Osteoblasts and osteoclasts are coordinated in a manner that the relation of bone forming and resorbing changes during lifetime. In the growth phase, bone formation exceeds bone resorption. These two opposite activities are in balance from the second to the fifth decade followed by a decline in bone formation, which mirrors in skeletal mass, strength and risk of fracture [2]. Moreover, it has been demonstrated that osteoclasts are regulated by osteoblasts and vice versa [10]. Their complex interactions are depicted in figure 4.
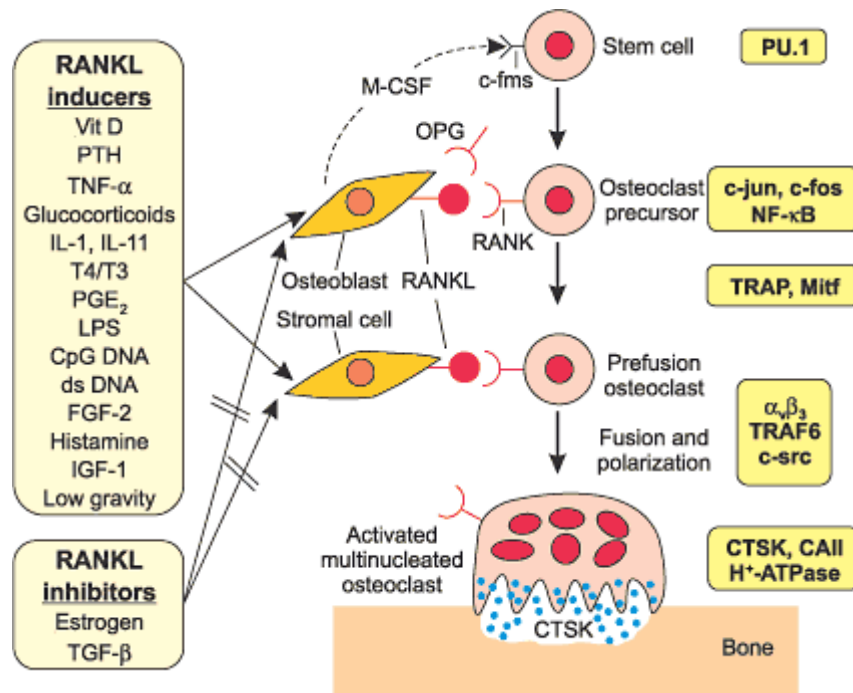
Figure 4: Coordination of osteoblasts and osteoclasts. M-CSF (macrophage colony stimulating factor) and OPG (osteoprotegerin, a soluble receptor for RANKL) are secreted by osteoblasts and regulate osteoclast function. RANKL (RANK-Ligand) is a membrane bound molecule of osteoblasts, which can interact with RANK (receptor activator of NF-kB) of osteoclasts. TGF-ß (transforming growth factor-beta), released from the bone matrix, attracts osteoblasts to the place where bone destruction has taken place. Hormones are actively participating in regulation of bone like PTH (parathormone), calcitonin (active vitamine-D hormone) and sexual hormones (estrogens). It is remarkable, that estrogens decrease osteoclast development and activity, in men and women [10].

Osteocytes arise from osteoblasts and are embedded in mineralized bone matrix. Lakunae (tiny spaces in the calcified matrix), in which osteocytes are localized, mediate cell communication via gap junctions and permit nutritional and metabolic diffusion with the blood vessels that traverse the present impermeable extracellular matrix [2] (figure 5).
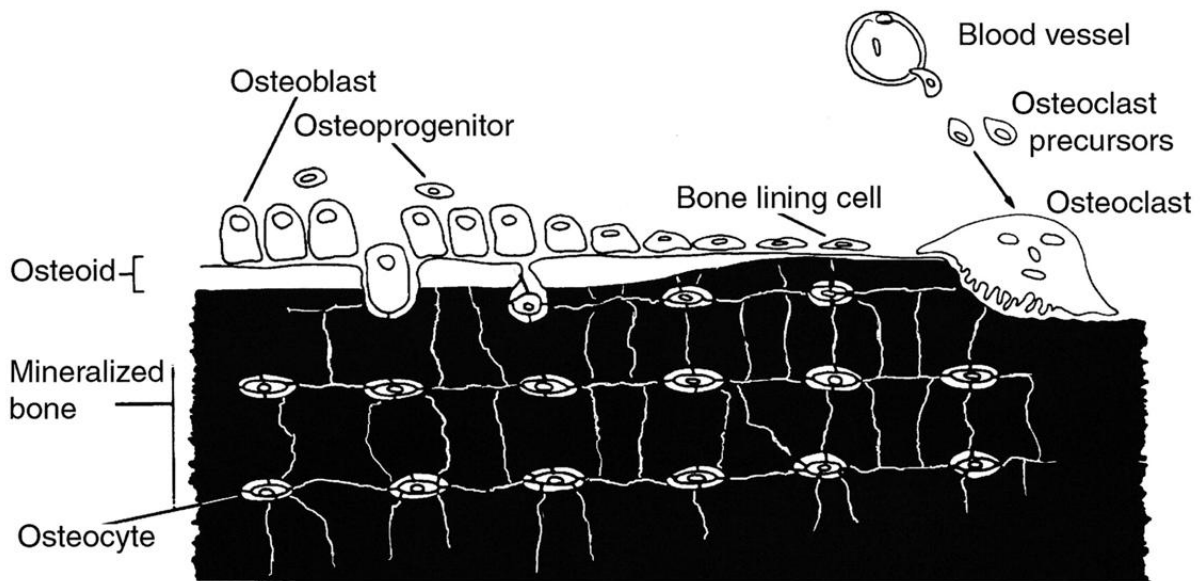
Figure 5: Localization of bone cells. Inactive osteocytes surrounded by mineralized bone. On top, a layer of collagen (osteoid), produced by osteoblasts. Efficient bone formation is always accompanied by bone resorption accomplished by osteoclasts.

1.1.4   Osteogenesis: Desmal and Endochondral Ossification

Formation of the skeleton can occur in two ways:

- Intramembranous ossification: differentiation of mesenchymal stem cells directly to osteoblasts.

- (Endo-) chondrale ossification: mesenchymal stem cells differentiate first to chondroblasts. Their produced cartilagous model is fundamental for further development of bone.

Direct osteogenesis occurs during embryonic development. It is responsible for the formation of the cranial vault, parts of the mandibula and clavicula and takes course as follows: mesenchym (primitive connective tissue) condenses and differentiates to osteoblasts. After producing the osteoid, minerals are deposited and osteocytes emerge. Osteoblasts, which are lying in the periphery next to the mineralized osteoid, deposit new bone tissue on the already existing bone trabeculae (appositional

growth). Finally, trabeculae grow together and build up the primary spongiosa that can be gradually turned into the compacta. In long bones, desmal ossification is found in the diaphysis, where osteoblasts arise in the perichondrium, building up the periost instead, responsible for the growth in width.

Indirect (endochondral) osteogenesis happens more often in the human body and is found in long bone formation, growth and healing.

Long bone growth (interstitial growth) is achieved with the epiphyseal plate/growth plate, lying between the epiphysis and metaphysis and constisting of a resting, proliferation, maturation, hypertrophy and mineralization zone [2] (figure 6).
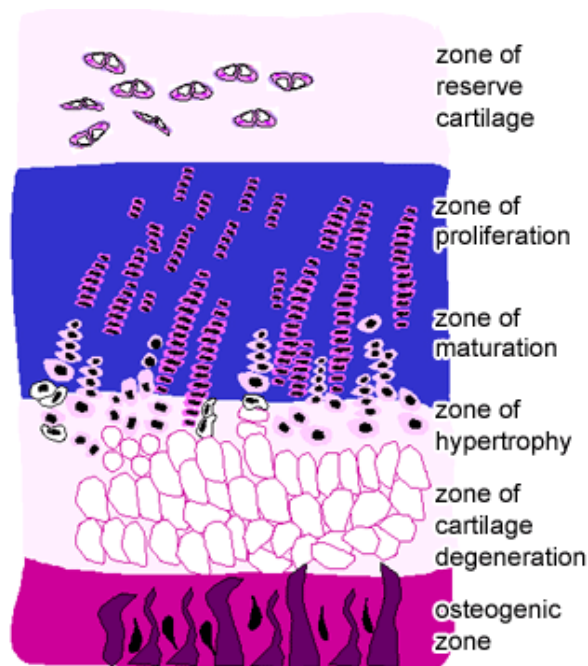
Figure 6: Schematic presentation of growing bone. In the reserve zone, undifferentiated chondrocyte progenitors are localized. These cells proliferate and generate a typical column structure. In the next zones, cells mature and hypertrophy (increase in size due to absorption of water). After destruction of the hypertrophied cell by chondroclasts, osteo-progenitor cells migrate into the left calcified cartilage anlage over the blood vessel system for bone formation [10].

1.1.5   Fracture Healing

Histologically, fracture healing is classified in primary (direct) and secondary (natural) bone recovery.

<u>Primary bone healing:</u>
Direct bone healing occurs, if the bone gap has a minimal size (<1mm) so that mesenchymal stem cells can differentiate directly to osteoblasts. This can happen naturally or can be achieved with the help of osteosynthesis [10].

<u>Secondary bone healing:</u>
Natural bone healing can be divided into three main phases (figure 7):

1) Reactive phase: bone injury associated with harmed blood vessels, soft tissue, bone matrix and bone cells activate the blood coagulation cascade for the formation of a haematoma. Incorporated cells of this blood clot die with the exception of fibroblasts. These cells survive and proliferate to form with recruited chondroblasts a so-called "soft callus" (fibro-cartilagous callus). After monocytes have infiltrated the harmed tissue, they differentiate to macrophages to remove destroyed tissue and cells.

2) Reparative phase: periost and endost in the fracture areal react with intensive proliferation of pre-osteoblasts. With blood vessels mesenchymal stem cells migrate inside, generating new bone tissue (woven bone) by means of desmal and chondral ossification.

3) Remodelling phase: after about 4 months, spongy bone gets gradually remodelled to lamellar bone [12].

Figure 7: Mechanisms and phases in fracture healing. First, a haematoma is formed to fill the gap, followed by generation of a fibro-cartilagous callus, which gets gradually remodelled to bone tissue [10].
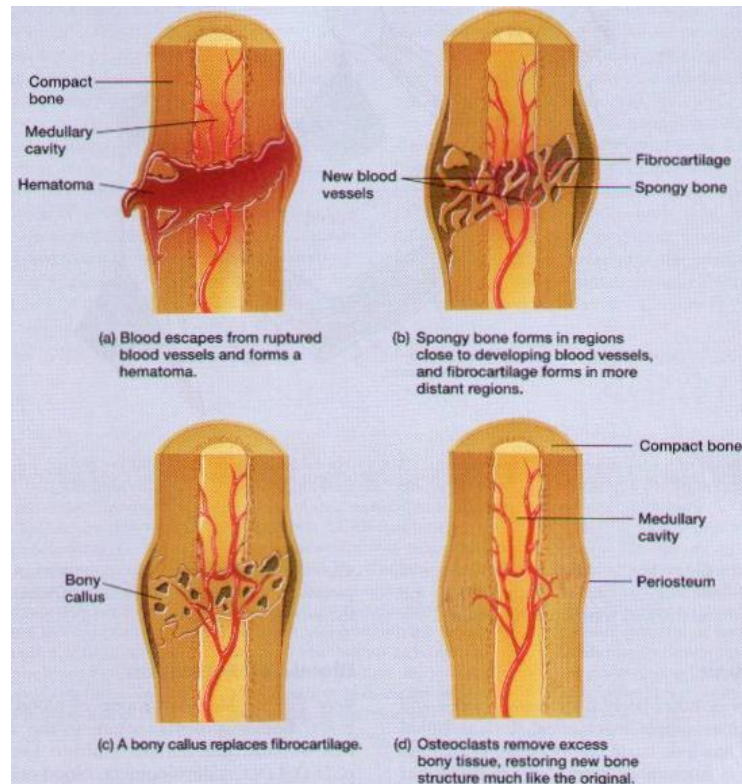
1.2 Bone Morphogenetic Proteins

1.2.1 Introduction

Bone morphogenetic proteins (BMPs) are members of the transforming growth factor -beta (TGF-ß) superfamily, which is composed of over forty members (like activins, inhibins, myostatins, nodals) and fundamentally important in cellular behaviour (such as proliferation, differentiation, tissue morphogenesis) [13]. BMPs were already discovered 1965 as purified extract of decalcified bone and have shown their potential as bone inductive proteins when implanted in animals and humans [14],[15]. These growth factors have been intensively studied, especially for bone healing and to date, more than 20 types of BMPs have been detected [16].

BMPs	Known Functions	Gene Locus
BMP1	BMP1 does not belong to the TGF-β family of proteins. It is a metalloprotease that acts on procollagen I, II and III. It is involved in cartilage development.	8p21
BMP2	Acts as a disulfide-linked homodimer and induces bone and cartilage formation. It is a candidate as a retinoid mediator. Plays a key role in osteoblast differentiation.	20p12
BMP3	Induces bone formation.	14p22
BMP4	Regulates the formation of teeth, limbs and bone from mesoderm. It also plays a role in fracture repair.	14q22-q23
BMP5	Performs functions in cartilage development.	6p12.1
BMP6	Plays a role in joint integrity in adults.	6p12.1
BMP7	Plays a key role in osteoblast differentiation. It also induces the production of SMAD1. Also key in renal development and repair.	20q13
BMP8a	Involved in bone and cartilage development.	1p35-p32
BMP8b	Expressed in the hippocampus.	1p35-p32
BMP10	May play a role in the trabeculation of the embryonic heart.	2p14
BMP15	May play a role in oocyte and follicular development.	Xp11.2

Table 1: Family of BMPs. According to sequence homology BMPs can be divided into following subgroups: Subgroup 1: BMP2, BMP4; Subgroup 2 (osteogenic proteins): OP1: BMP5, BMP6, BMP7; OP2: BMP8; Subgroup 3: BMP3 (osteogenin) [17]–[19].

BMP-2, -3, -4, -5, -6 and -7 are expressed during bone healing. Nevertheless, BMP4 seems to be unessential in bone formation as shown in mice in which the lackage of BMP4 didn't affect skeletogenesis and fracture healing. In contrast, BMP2 is indispensable and associated with spontaneous natural incurable fractures in the limbs [20]. BMP3 inhibits the potential of BMP2 to induce differentiation of osteogenic progenitor cells to osteoblast, thereby highly affecting bone mass volume. Furthermore it has been shown that trabecular volume was doubled in BMP3 deficient mice compared to wild type animals [21].

TGF-ß/BMP signaling is accomplished by interaction of two kinds of receptors: type I receptors (BMPR-IA (ALK-3), BMPR-1B (ALK-6), ActR-1A (ALK-2)) and type II receptors (BMPR-II, ActR-II, ActR-IIB). In contrast to ActR, which are also activated by activins, BMPRs are triggered by BMPs only [22].

1.2.2   Structure and Signaling

BMPs are synthesized as long precurser proteins. These proteins are proteolytically cleaved at an Arg-X-X-Arg consensus sequence to form mature dimers. Connection of polypeptid chains via a single disulfide bond can form homodimers or heterodimers, indispensable for BMP signaling. 3D structure of BMP7 (figure 8 left) shows three disulfide bonds, a cysteine knot (protein core) and 5 anti-parallel ß-sheets, which originate from the central point creating two finger-like projections [23]–[25].
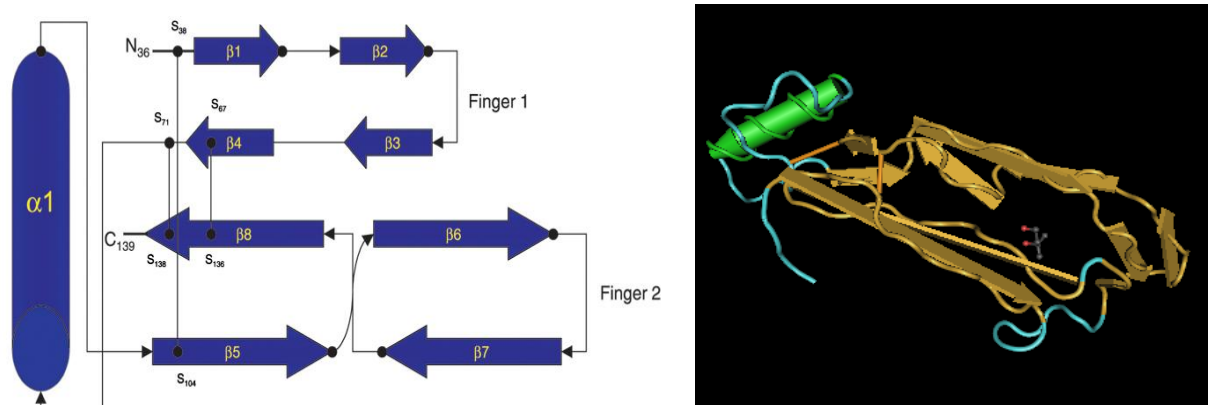
Figure 8: Schematic tertiary structure of BMP7 (left) and 3D structure of BMP2 (right).

BMP-dimers bind to specific BMP type I and BMP type II receptors (serine/threonine kinase receptors) on the cell membrane, which in turn leads to phosphorylation of downstream Smad proteins. Activated R-Smads (such as Smad1, Smad5, Smad8) form dimers with a co-Smad (Smad4) followed by translocation into the nucleus to function as trancriptional activators and regulators of gene expression of diverse additional transcription factors, important in osteogenesis [13]. Perturbance of the signaling can be mediated by so called inhibitory Smads (Smad6, Smad7) that interrupt complex formation of R–Smads with co-Smads or prevent receptor activation [26] (figure 9).
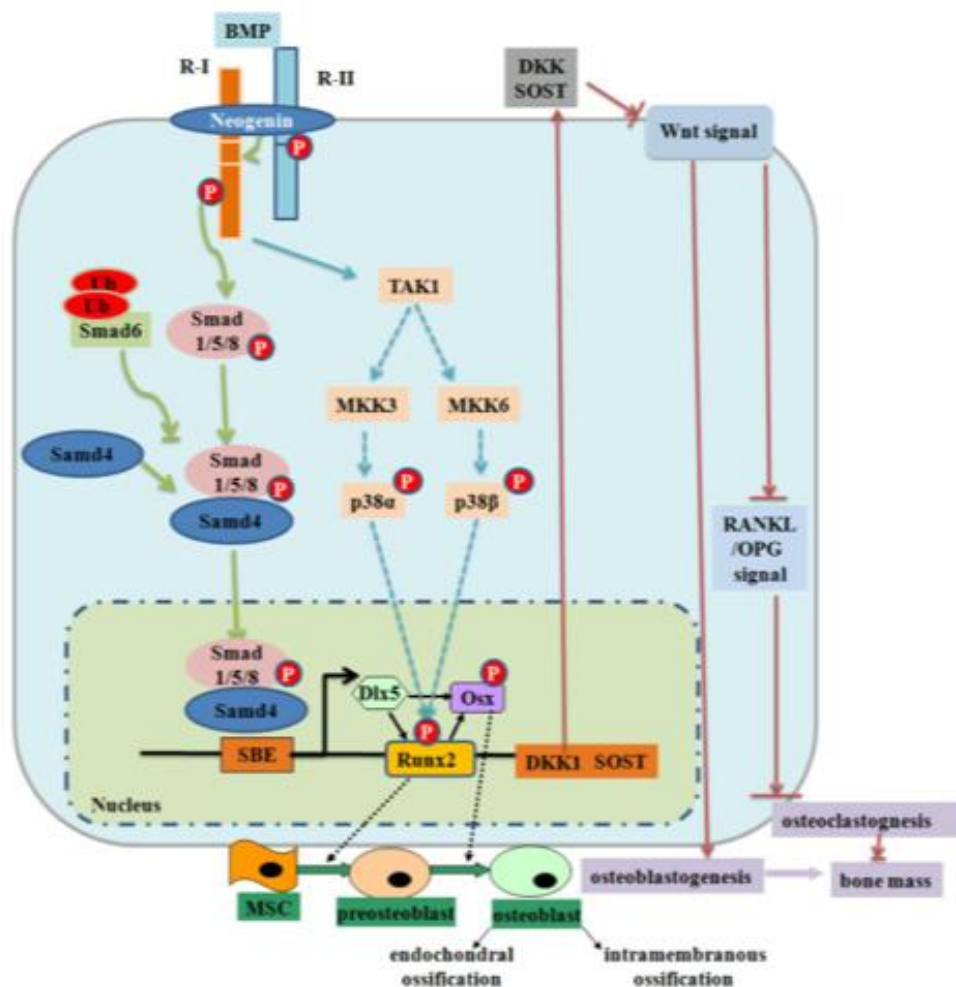
Figure 9: BMP signaling and regulation in osteoblasteogenesis. BMP induced receptor activation switches on the Smad-dependent pathway on the one side, MAPK-pathway on the other side, both intervening in bone formation by triggering target gene expression (Dlx5, Runx2, Osx). Smad6 interfere with BMPR-I and inhibits activation of R-Smads (Smad1, 5, 8). As pictured, primary Dlx5 expression followed by Runx2 and Osterix activation, direct MSCs to osteoblast lineage. DKK1, as well as Sost, produced in these two pathways, block canonical Wnt signaling, important in osteoblastogenesis. SBE: Smad-Binding-Elements, P: phosphorylation, Ub: ubiquitination

Differences in biological activity of BMP2/7 heterodimers in contrast to homodimers have been observed in several studies over the last years [8], [27], [28]. In order to explain how heterodimers can enhance receptor activated signaling, two most prominent theories have been established. A possibility is that the combined activation of ALK3 and/or ALK6 by BMP2 with ALK2 by BMP7 [29]–[31] leads to a higher phosphorylation of downstream lying Smad1/5/8 proteins. Higher activation of the signaling pathway mirrors in enhanced ALP activity and osteoblast differentiation [32]. In the second theory, BMP inhibitors explain these results. There, it is suggested that homodimers induce the synthesis of its antagonists to a higher extent and/or their activity is more affected by them. In this regard, heterodimeric BMPs lead to a lower Noggin expression compared to homodimeric BMPs in C2C12 cells. Furthermore a decrease in BMP2/7 signaling/activtity could not be detected after treatment of this BMP inhibitor [33]. In order to verify one of these concepts, further investigations of BMP signaling and expression levels and affinities of its antagonists are necessary [34].

1.2.3   Transcription Factors in Osteoblastogenesis

Sox (SRY-related high mobility group box) genes are characterized by their specific high mobility group box domain, RPMNAFMVW, a DNA binding domain involved in DNA-dependent processes [35]. One of them is Sox9, a transcription factor, expressed at the beginning of the skeletal development involved in mesenchym condensation. It was detected in osteoblast- and chondroblast-progenitor cells and is expressed before Runx2 [36]. Sox9-homodimer can bind to Col2a1 enhancer, as well as L-Sox5 (the large Sox5 isoform) and Sox6 homo/heterodimer, all together regulating indispensable steps (expression of Col2a1 and aggrecan) in chondrogenesis (in the epiphysis plate) [37], [38].

Runx2 (Cbfa1) belongs to the Runt domain family of transcription factors and is a master organizer of gene expression in mature and unmature osteoblasts. It binds to specific DNA sequences. Thereby, it directly regulates their expression and furthermore interacts with several transcription factors, co-repressors and co-activators operating indirectly on their target gene expression [39]. Runx2 is an early

factor expressed during osteogenesis and can be used as reliable marker for bone formation [40].

Runx2 is essential in proper embryonic development for condensation and differentiation of MSCs to osteoblasts, for chondrocyte hypertrophy and for vascularization in skeleton formation. A complete absence of ossification was shown in Cbfa1 deficient mice [41], [42]. On the contrary, overexpression of this gene in already lineage determined osteoblasts results in blockage of terminal differentiation and augmentation of bone resorption (probably increased levels of osteoclast activations due to higher RANKL expression), indexing that the molecular mechanisms have to be tightly regulated for proper function [43]. Mutations in Cbfa1 in human can be the reason for cleidocranial dysplasia, an autosomal dominant disease [44].

Osterix, the mouse homologue of human specificity protein-7, is a zinc finger containing transcription factor and downstream target of Runx2/Cbfa1 [45]. It regulates the expression of genes employed in development of pre-osteoblasts in mature osteoblasts and osteocytes [46]. In Runx2 deficient mesenchymal cell lines Osterix could be produced after treatment with BMP2 via Msx2, a homeobox gene, and only after a knockdown of this transcription factor, Osterix expression was repressed. Therefore, it is suggested that its expression can be Runx2 dependent or independent [47]. Osterix's crucial role in bone development has been determined in mice, where lackage/loss of Osterix prevents bone formation, inhibits chondrogenesis and leads to an absence of osteoblasts. Moreover other osteoblast markers, among them osteonectin, osteopontin and osteocalcin, failed to be expressed [48].

1.2.4 Timeline of Molecular Events

First, Sox genes (Sox9) are expressed, which are primarily required for the entrance of MSCs into the osteogenic/chondrogenic lineage [49].

In the next step, Runx2 is required in combination with Osterix (almost exclusively expressed in osteoblasts) for the commitment to osteoblasts instead of chondroblasts [48]. After the cell fate has been determined, Runx2 is downregulated under an unknown mechanism to enable immature osteoblasts to evolve to matrix producing osteoblasts. ATF4 (activating transcription factor 4), expressed throughout the whole process, is suggested to be employed in terminal differentiation hence lackage of this factor in mice is associated with reduced bone mass [50].

Osteogenic/Chondrogenic cells entering the chondrogenic way have L-Sox5 and Sox6 expressed in addition to Sox9 in order to become chondrocytes. To prevent premature hypertrophy, Runx2 has to be downregulated by Sox5 and Sox6 (via an unknown mechanism) or via repression of ß-catenin to become in turn osteoblasts [49]. Later, when hypertrophy is desired, Runx2 and Runx3 are expressed followed by transformation to osteoblasts by cMaf expression, the only known factor involved in this step [51].

1.2.5 Cross-talk of Signaling Pathways

Apart from already mentioned transcription factors (such as Sox, Runx, Osx, ATF4) and osteoinductive TGF-ß/BMP signaling, bone formation is stimulated by a variety of growth factors like insulin-like growth factor (IGF), platelet-derived growth factor (PDGF), vascular endothelial growth factor (VEGF) and fibroblast growth factor (FGF). These factors are involved in chemotaxis, proliferation and differentiation and coincide in the MAPK-pathway, with the exception of VEGF [52], [53]. As depicted in figure 10, additionally Wnt- and Hedgehog signaling pathways are involved in bone formation [52].

It has been shown, that BMP2 increases nuclear ß-catenin level in pre-osteoblast cells, an essential component of canonical Wnt signaling. Due to resulting expression of several Wnt genes (Wnt15, Wnt3a, Wnt7, Wnt5b), an interconnection between BMP and Wnt signaling is suggested [54], [55] (figure 10). Disruption of ß-catenin dependent Wnt signaling is associated with several diseases, from abnormalities in bone mass to cancer and Alzheimer`s disease [56], [57]. While Wnt1 and Wnt3a turn on the canonical pathway involved in cartilage formation, Wnt5a activates non-canonical Wnt signaling causing terminal activation of NFAT [55] (nuclear factor of activated T-cells), a transcription factor important in immune responses [58].

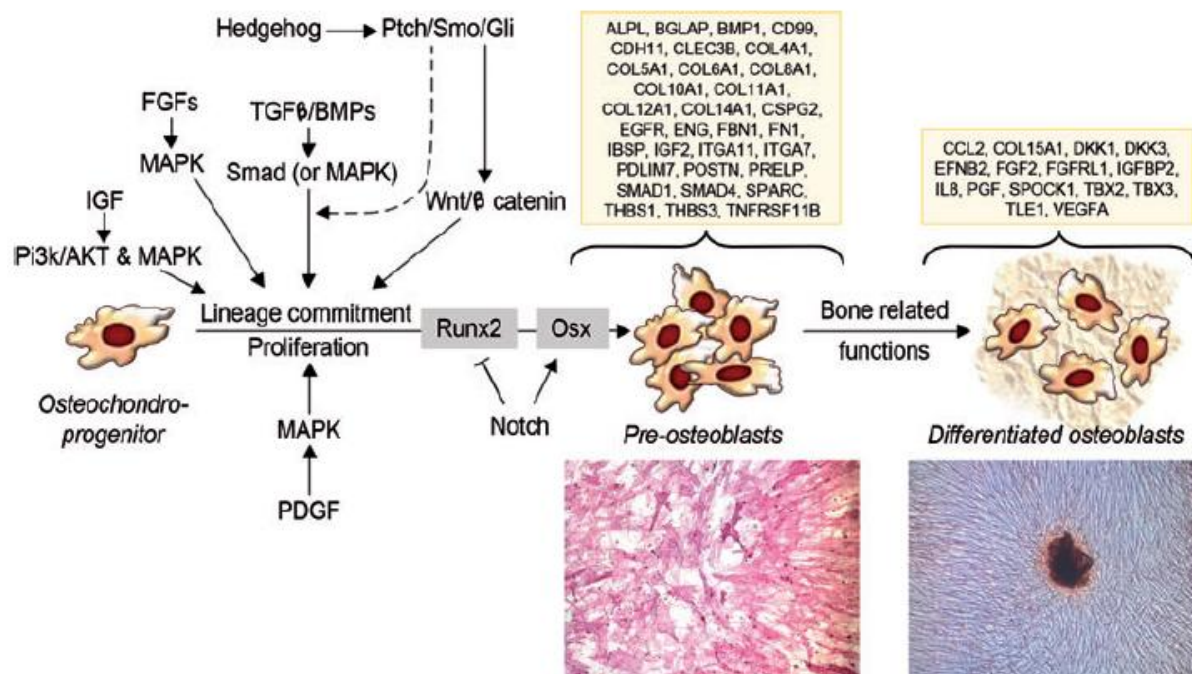
Figure 10: Cross talk between signaling pathways (TGF-ß-, MAPK-, Wnt-, Hedgehog-, Notch-, FGF-signaling) and transcription factors. Growth factors stimulating expression of bone related genes, partially antagonized or enhanced by Notch, dependent on the point of action. Boxes represent significantly upregulated genes in pre-osteoblasts and differentiated osteoblasts (mineral depositing cells).

1.2.6 Negative Regulation of BMP Signaling

Antagonists, among them noggin, chordin and follistatin have been reported to bind extracellular to bone morphogenetic proteins to prevent receptor activation [reviewed in 59]. These BMP interacting proteins have convinced their necessity in normal embryonic and postnatal development in many studies. A balance between BMP and BMP antagonists is crucial for efficient bone remodelling and is interestingly achieved by the BMPs' ability to regulate the expression of their antagonists. Recent clinical approaches are under investigation showing that different ratios of BMPs to its antagonists are present in unions compared to non-unions, suggesting that this may be a target for efficient bone healing in human [60].

1.2.7 Clinical Applications of BMPs

BMPs are the molecules that have been most intensively studied in experimental and clinical applications for bone regeneration. Especially, BMP-2 and BMP-7, have convinced in their potential in bone tissue engineering, licensed in the clinics since 2001 (BMP2) or 2002 (BMP7) [61]. Unfortunately, the necessary high dosages of these proteins (up to milligrams) are associated with high economic costs and potential systemic side effects. Therefore the discovery of endogenous BMP2/7 co-expression, characterised by a significantly lower effective dose or higher osteoinductive stimulus compared to the same homodimer concentration *in vitro* and *in vivo*, seems to show great promise in the future [27].

1.3 Biomaterials

1.3.1   Specific Biomaterials in Bone Tissue Engineering

A variety of scaffolds have already been used, in principle categorized in naturally derived polymers like chitosan, fibrin, fibroin, agarose and synthetic polymers such as PLA and PGA. Natural polymers show low toxicity, have good biocompatibility and are degradable which is essential for a good biomaterial. Synthetic biomaterials have similar features but with the big deficit that they only possess low biocompatibility. They release toxic products (for instance in the case of PGA and PLA, two polymers that are often used in bone regeneration) during degradation and are not bioactive (beneficial interaction of the biomaterial with the surrounding tissue). Scaffold materials have to be optimized in pore distribution, pore size and exposed surface area for regulation of cell migration, proliferation and production of extracellular matrix for nutrient accessibility and waste removal [reviewed in 62].

1.3.2   Fibrin as Biomaterial for Bone Tissue Regeneration

Fibrin hydrogels are natural polymers that are usually produced during blood coagulation. Fibrin exists in two isoforms, a low- (305kDa) and a high-molecular-weight fibrinogen (340 kDa), which differ in rate of cell growth, cellular infiltration and clotting rate (figure 11). In general, fibrin regulates cell migration, adhesion, proliferation and vessel formation [reviewed in 63]. Fibrin gels can be easily formed by combining fibrinogen with thrombin, which mediates proteolytically a gelation reaction of fibrinogen to fibrin (figure 12). Fibrinogen, the fibrin-precurser protein, can be isolated from the patient's own blood to eliminate the risk of immune rejections and by reason of its variety of advantages, fibrin sealants have already been used as a scaffold alone or coupled with cells and bioactive agents in wound healing [64]. Additionally, fibrin biomaterials have been used as gene-activated matrices for sustained release in protein- and drug-delivery and is of interest for tissue regeneration due to its promising features [64], [65].

1.3.3   Fibrin and Fibrinogen Structure
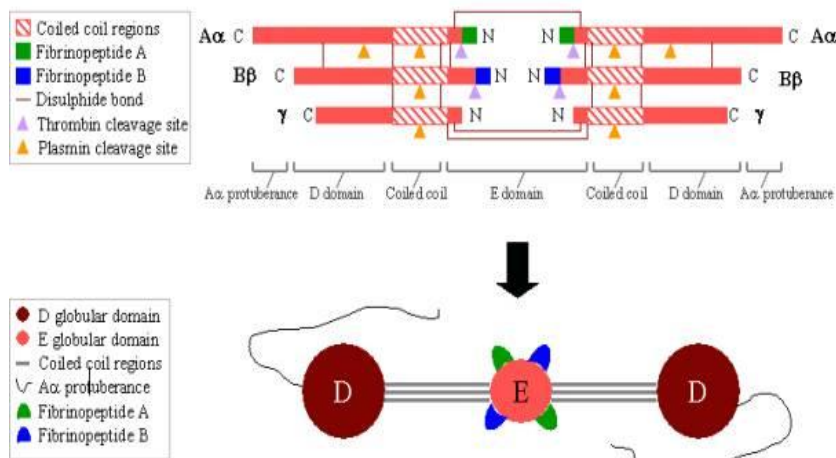
Figure 11: Fibrin and Fibrinogen structure: Fibrinogen is a hexamer composed of two alpha (Aα,), and two beta (Bβ) and two gamma (Cγ) peptide chains [66]. Fibrinogen is converted to fibrin by proteolytic cleavage of fibrinopeptide A and fibrinopeptide B. Fibrin monomers join spontaneously together by non-covalent and electrostatic forces to create a polymer structure [67].

E=central domain, coincidence of (all) N-terminal ends of peptide chains; Coiled coil region= consistent of one α, ß, γ respectively, connects E with D domain; D= globular form of C-terminal ends of peptide chains, where Aα protrudes to interact with each other and with E domain for fibrin cross-linking. Thereby, active Factor XIII acts as transaminase to stabilize polymer structure [66], [67].
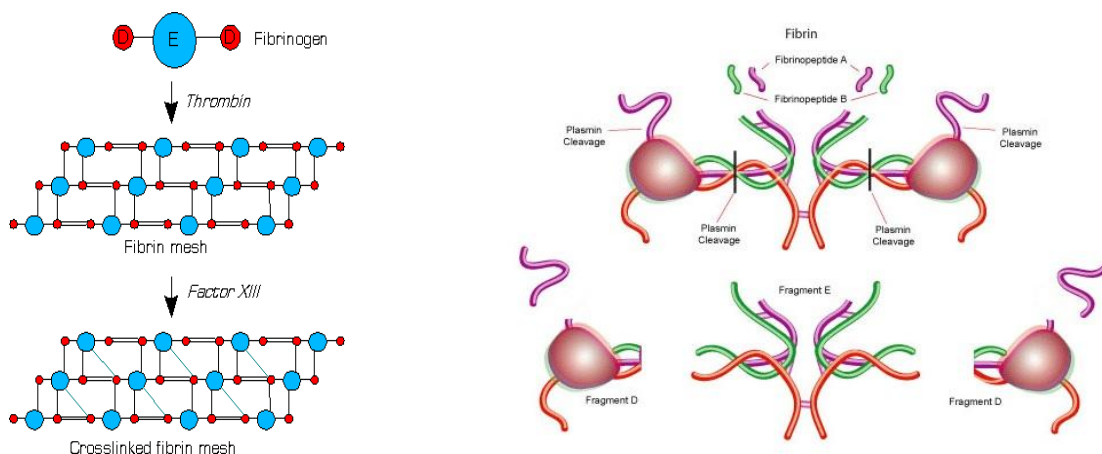
Figure12: Formation of a fibrin polymer (left), detailed structure of fibrin (right) after cleavage by thrombin or plasmin (proteolytic cleavage between E and D-domain for fibrinolysis).

1.4 Aims of the study

Considering the high incidence of deficient bone repair approaches after osteosynthesis in the clinics and inadequate results in bone tissue regeneration, the aim of this study was to:

1. Analyse and compare the behaviour of mesenchymal stem cells (MSCs) after treatment with different kind of osteogenic stimuli (osteoinductive medium, rhBMP2, pVax-BMP2/7)

2. Demonstrate the suitability of fibrin as biomaterial for MSCs as well as to demonstrate its feasibility as gene activated matrix for bone tissue engineering *in vitro.*

2 Material and Methods

2.1 Molecular Biological Methods

2.1.1 Plasmids

All Plasmids used in this study were either self designed (pVax-Wnt5a, pVax-Wnt7a, pVax-BMP2/7) or purchased [pmaxGFP from Amaxa (, Cologne, Germany); pVax backbone from Life Technologies (Paisley,UK, #260-20)] .

Figure 13: Vector map indicating CMV-promoter for constitutive maxGFP-expression, kanamycine resistance gene (KanR) and origin of replication (puC-Ori).

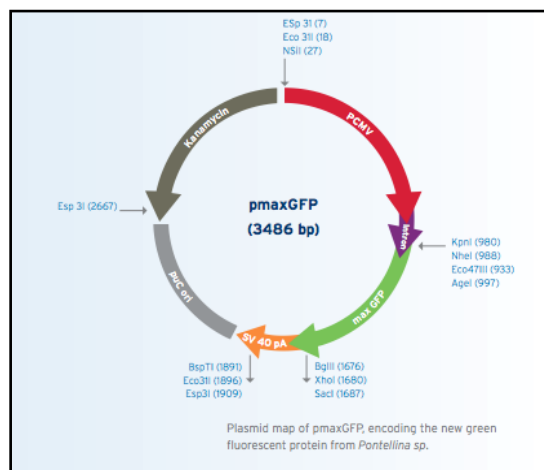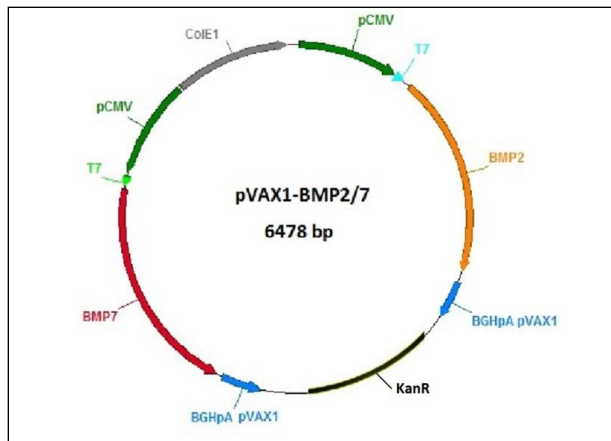Figure 14: Vector map of pVax-BMP2/7. Co-expression plasmid carrying BMP2 and BMP7 in inverted orientation. BMP2 cDNA sequence, BMP7 cDNA sequence, E. *coli* origin of replication (Col E1), bi-directional CMV promotors (pCMV), bovine growth hormone poly adenylation signal (BGHpA) and kanamycine resistance gene (KanR) are shown. In the present study, two different preparations of pVax-BMP2/7 were used for the osteogenic differentiation in 2D and 3D.

2.1.2   Cloning with the Gateway® System

Wnt genes (Wnt5a and Wnt7a) located in pCR8 entry vectors were cloned into GW8.4 destination vector by homologous recombination event of the flanked att sites. LR Clonase™ II Enzyme Mix (Gateway®LR Clonase II Enzyme, Invitrogen, Germany) was used, containing the bacteriophage lambda recombination protein Integrase (Int) and Excisionase (Xis), the E.*coli* encoded protein Integration Host Factor (IHF) and reaction buffer.

LR-Reaction:
150 ng pCR8-Wnt5a/7a
150 ng GW8.4
4 µl LR Clonase™ II Enzyme Mix
ad 18 µl TE buffer, pH 8.0

The recombination was performed at room temperature for one hour and terminated by adding 1µl Proteinase K (2µg/µl, provided in the kit,10 minutes, 37°C).
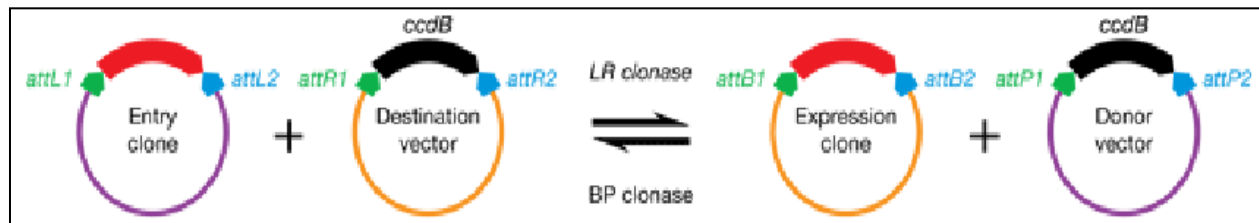
Figure 15: Gateway system. Entry vector (pCR8) carrying Wnt target gene and spectinomycine resistance gene; destination vector (GW8) provided with ccdB gyrase blocker and kanamycine resistance gene.

2.1.3   Sequencing

Sequencing was performed by Microsynth. A T7 backbone primer was used for sequencing of the constructs pVax1-Wnt5a and pVax1-Wnt7a.

Reaction:
0.8 µg Plasmid
ad 10 µl ddH$_2$O

seq T7: 5'-TA ATA CGA CTC ACT ATA GGG -3'

2.1.4   Agarose Gel Electrophoresis

Separation of DNA and RNA-fragments was generally achieved using 1% agarose gels. Ethidiumbromid (0.03 µg/ml) was added to the liquid agarose for detection of the nucleic acid-fragments. Unless described otherwise, gels were run with 200V for 20 minutes. DNA Markers were used to determine the size of the products. Loading buffer was mixed with the template prior loading on the gel. For fragments smaller than 1000bp, XCFF loading buffer was used, whereas for larger fragments BPB was added instead. UV-light was used for detection; photos were taken with a CCD camera.

20x SB-Buffer (pH8, 1l)	
8 g NaOH	10 mM
35 g boric acid	28.3 mM

6x BPB loading buffer	
bromphenol blue	0.025%
glycerol	30%
ddH$_2$O	70%

6x XCFF loading buffer	
xylene cyanole FF	0.025%
glycerol	30%
ddH$_2$O	70%

Ethidium bromide (EtBr) Stock solution : 10 mg/ml in ddH$_2$O (Sigma-Aldrich, Vienna, Austria)

DNA markers:

Quantitas Fast 100bp-2kbp (Biozym, Hessisch Oldendorf, Germany)

FastRuler^{TM} low range DNA ladder: 100bp-1kbp ladder (Thermo Scientific, Carlsbad, USA)

FastRuler^{TM} high range DNA ladder: 1-10kbp ladder (Thermo Scientific, Carlsbad, USA)

Low range DNA ladder

High range DNA ladder

Quantitas Fast DNA Marker: 100bp - 2Kb
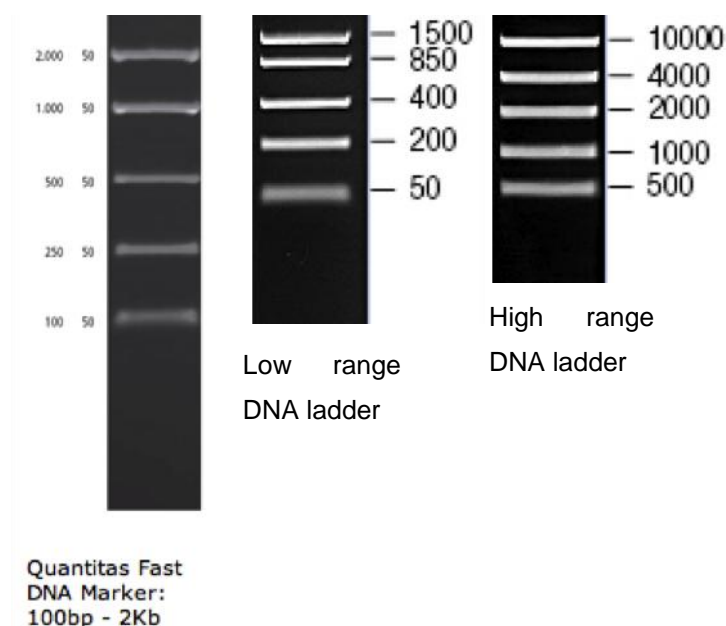
2.1.5   DNA Extraction from Agarose Gels

After gel electrophoresis, desired bands were cut out of the agarose gel with a scalpel and transferred to sterile pre-weighed Eppendorf tubes. For DNA purification, 10 µl membrane binding solution per 10 mg agarose gel was added which was supplied by Wizard®SV Gel and PCR clean Up kit (Promega, Madison, USA). Following steps were performed according to the instructions of the manufacturer.

2.1.6   DNA Cleavage with Restriction Enzymes

Restriction reactions were performed as recommended by the manufacturer. Incubation time was at least 2 hours at 37°C while shaking on a thermomixer. Verification of efficient restriction reactions was done by gel electrophoresis.

Restriction reaction:

2 µl   10x fast digest buffer green (Thermo Scientific, Carlsbad, USA)

1 µl   restriction enzyme (10 U/µl, Thermo Scientific, Carlsbad, USA)

1-5 µl plasmid-DNA (1-2 µg)

ad 20 µl ddH$_2$O

2.1.7   Ligation

The ligation system was used from Roche Diagnostics (Mannheim, Germany). The excised fragment was ligated into a previously linearized target vector. Different vector to insert ratios were performed (1:2, 1:3) after stochiometric ratios were estimated based on band intensities on the gel. Ligation reaction was accomplished at 4°C overnight.

T4 Ligation reaction:

2-3 µl Insert DNA

1 µl   Backbone (or Target) Vector

1 µl   10x ligation buffer

T4 Ligase (1 unit)

ad 10µl ddH$_2$O

2.1.8   Preparation of Competent E. *coli* Top10

100 ml of LB-medium was inoculated with 5 ml of overnight culture at 37°C while vigorously shaking. After E. *coli* reached an OD$_{600}$ of about 0.4, cells were transferred to a sterile 50 ml polypropylene tube and stored on ice for 10 minutes. Cells were centrifuged at 4000 rpm (4°C) and the pellets were resuspended with 30 ml of an ice-cold 80 mM MgCl$_2$ 20 mM CaCl$_2$ solution containing 10% glycerol. The cells were again centrifuged and the resulting pellet resuspended in 2 ml of an ice-cold 100mM CaCl$_2$ 10% glycerol solution. Obtained competent E. *coli* were aliquoted and frozen at -80°C for storage.

Culture Medium:

LB-Medium: 10 g tryptone
5 g yeast extract
10 g NaCl
ad 1 L ddH$_2$O

LB-Agar: 10 g tryptone
5 g yeast extract
10 g NaCl
15 g Agar
ad 1 L ddH$_2$O

2.1.9   Transformation of Plasmid-DNA in competent E. *coli* Top10

20 µl of ligation reaction was mixed with 20 µl competent E. *coli* and was incubated for 30 minutes on ice following heat shock at 42°C for 90 sec. After immediate incubation of the sample on ice for two minutes, 80 µl SOC medium was added. The cells were gently shaken at 37°C for one hour prior to plating on LB-agar plates containing appropriate antibiotics for subsequent selection of positive clones.

SOC medium	
tryptone	2%
yeast extract	0.5%
NaCl	10 mM
KCl	2.5 mM
MgCl$_2$	10 mM
MgSO$_4$	10 mM
glucose	20 mM

2.1.10 Identification of Positive Clones

Single colonies were picked from agar-plates and resuspended in 20 µl LB-medium. Colony-PCRs were performed followed by gel electrophoresis verifying an insertion of the gene of interest. One insert-specific and one vector-specific primer were chosen for identification of clones with right insert orientation. Positive clones were inoculated in 4ml LB containing appropriate antibiotics and cultured over night for subsequent plasmid preparation (mini preparation).

Colony PCR Reaction:

1 µl bacterial aliquot (containing bacteria of one colony resuspended in 20 µl LB medium)

0.5 µl (10 mM) dNTPs

2 µl (10 pmol) Primer (Primermix of insert- and backbone primer)

2.5 µl 10x buffer

0.2 µl (1unit) Hot-Taq Polymerase (PeqLab Biotechnologie Gmbh, Erlangen, Germany)

ad 25 µl ddH$_2$O

Colony PCR Program:

95°C	5 min	
95°C	30 sec	repeat
Ta	30 sec	25-30 cycles
72°C	1 min/1 kb	
72°C	10 min	
13°C	pause	

2.1.11   Preparation of Plasmid-DNA

Isolation of plasmid-DNA was performed by the Wizard$^{®}$ SV mini preparation kit obtained from Promega (Madison, USA). Plasmid isolation was done as recommended by the manufacturer. Mean yield of prepared plasmid-DNA was generally 20-30 µg.

Maxipreparation of plasmid-DNA was carried out using the Endotoxin-free Maxiprep kit (Qiagen, Hilden, Germany) according to the instructions of the manufacturer. Approximately 1 mg of purified plasmid-DNA was obtained.

2.1.12   RNA Isolation and DNA-Isolation with TriFast^{TM}

Rat adipose-derived mesenchymal stem cells, used in the study were incubated for 30 days for efficient osteogenic differentiation, prior resuspension with TriFast (Peqlab, Erlangen, Germany) for subsequent RNA-Isolation. For efficient cell lysis, 1 ml reagent was used for monolayer cells on 6 well plates, based on the area of the culture dish (9.6 cm^2). For 3D cell culture, an additional homogenization step (ball mill, time: 20 min, frequency: 30/s) was necessary to achieve complete breakdown of cells. In the next step, 200 µl sterile chloroform per 1 ml of TriFast^{Tm} was added, mixed by inverting for 15 seconds and centrifuged for 5 minutes at 12,000 x g for phase separation. RNA was located in the upper aqueous phase, while proteins and DNA were located in the lower phenol phase and interphase. RNA was transferred to a new sterile Eppendorf tube and stored on ice. Subsequent RNA precipitation was achieved by a further centrifugation step after applying 0.5 ml isospropanol per 1 ml of TriFast^{Tm} to the RNA. The RNA pellet was washed with sterile 75% ethanol by vortexing and centrifugation for 5 minutes at 12,000 x g (4°C). Finally, the RNA pellet was resuspended in ddH$_2$O after air-drying for 5 to 10 minutes removing excess of ethanol. RNA concentration was quantified with UV-spectroscopy.

DNA was isolated by taking the upper phase and interphase (DNA) following DNA precipitation by mixing 2 volumes 10% Ethanol and 0.1 volumes 3 M NaAc to one volume of DNA and storing for one hour at -80°C. After centrifugation with 13,000 x g

for 15 minutes (4°C), the obtained DNA pellet was resolved in 250 µl resuspension solution applied in Wizard® SV minipreparation kit (Promega, Madison, USA). DNA was purified following the instructions of the manufacturer.

2.1.13   Determination of RNA Quality and Quantity

After RNA-Isolation, RNA concentration was determined by measuring the ratio $A_{260/280}$ with UV-spectroscopy (SmartSpec^{Tm}3000, Bio-Rad, Berkely, USA). An A_{260} of 1.0 corresponds to 40 µg/ml of RNA or 50 µg/ml of DNA. RNA concentration was measured with a 1:100 dilution in a quartz cuvette. Values for $A_{260/280}$ between 1.70 and 2.0 indicated pure nucleic acid with minimal protein contamination, suitable for reverse transcription into cDNA. Additionally RNA-gels were made to exclude contamination with nucleases during previous processing steps.

2.1.14   cDNA Synthesis

RNA was reverse transcribed into cDNA with AMV reverse transcriptase purchased from Promega (Madison, USA). DNaseI/AluI (Promega, Madison, USA; Thermo Fisher Scienitific, Waltham, USA) digestion was performed, in order to obtain pure mRNA. After DNA digestion at 37°C for 30 minutes, 1/10 volume Stopping Solution, 1/10 volume 3 M NaAc and 2.5 volume ice-cold 100% ethanol were applied for RNA precipitation at -80°C overnight.

The samples were then centrifuged with 14,000 x g for 50 minutes (4°C) and the pellets were washed with 1 ml ice-cold 70% ethanol (5 min 13,000 x g 4°C). After air-drying the pellets for about 10 minutes, the RNA was dissolved in 10 µl oligo dT$_{18}$ ddH$_2$O solution (1:20). After 10 minutes of denaturation at 70°C, oligo dT$_{18}$ primers were annealed on ice. AMV-RT reaction mix was added and cDNA-synthesis occurred in a thermocycler. Incubation at 42°C was performed for 1 hour and subsequent synthesized cDNA was separated from the RNA by incubation for 5 minutes at 95°C. The cDNA was diluted with 80 µl ddH$_2$O to a final concentration of 10 ng/µl. For real-time PCR, 4 µl of these solutions (40 ng DNA) were used as templates.

DNaseI/ AluI digestion reaction (20 µl)	
RNA	1 µg
10x DNase-buffer	2 µl
DNaseI	1 µl
AluI	1 µl
ddH$_2$O	up to 20 µl

AMV-RT reaction mix (10µl)	
10x AMV-buffer	2 µl
dNTPs	2 µl
AMV-RT	1 µl (20 units/µl)
ddH$_2$O	5 µl

2.1.15 qPCR

cDNA levels were quantified using C1000^{TM} Thermal Cycler and CFX Manager^{TM} (Bio-Rad, Berkely, USA). qHPRT (hypoxanthine-guanine phosphoribosyltransferase) served as reference control (house keeping gene) for analysing the expression of following osteogenic markers: Osteocalcin (OC), alkaline phosphatase (ALP), sialophosphoprotein I (SPP I), collagen type I (Col I). By means of 2^-d(Ct) formula, expression values were generated for comparison.

qPCR Reaction:

10 µl KAPA^{TM} SYBR$^®$ Fast qPCR Mastermix (2x)

0.4 µl Primermix (200 nM)

4 µl Template (40 ng)

ad 20 µl ddH$_2$O

qPCR Program:

95°C	3 min	
95°C	10 sec	repeat
Ta	30 sec	39 cycles
72°C	10 sec	
95°C	10 sec	
60°C	30 sec	

2.1.16   Primer

Lyophilised primers purchased from Microsynth (Switzerland) were diluted in ddH$_2$O to a final stock concentration of 100 µM and used in a final working concentration of 200 nM for real-time-polymerase chain reaction. Optimal annealing temperatures were identified by temperature gradients. All primers depicted in table 2 were designed with beacon designer (Premier Biosoft).

Primer	Sequence	T$_A$
mrHPRTs	5'-CTC TCA ACT TTA ACT GGA AAG A-3'	60°C
mrHPRTas	5'-TCT GGA ATT TCA AAT CCA ACA-3'	60°C
qOCs	5'-CCT AGC AGA CAC CAT GAG-3'	60°C
qOCas	5'-CTT GGA CAT GAA GGC TTT G-3'	60°C
qBMP7(vec)s	5'-GAT AGC CAT TTC CTC ACC-3'	52.7°C
qBMP7(vec)as	5'-GAA CTC TCG ATG GTG GTA-3'	52.7°C
maxGFPs	5'-ATG ACC AAC AAG ATG AAG AGC A-3'	52.5°C
maxGFPas	5'-GTA GGT GGC GAA GTG GTA GAA G-3'	52.5°C
qSppIs	5'-GAC CCA TCT CAG AAG CAG AAT CT -3'	55°C
qSppIas	5'- GAC CCA TCT CAG AAG CAG AAT CT-3'	55°C
qCola1s	5'-AGC GGA GAG TAC TGG ATC GA-3'	55°C
qCola1as	5'-ATG TAC CAG TTC TTC TGA GGG CAC -3'	55°C
qALPs	5'- AGG GTG GAC TAC CTC TTA GGT CT-3'	55°C
qALPas	5'- CGT GGT CAA TCC TGC CTC TT-3'	55°C
Oligo dT18	TTTTTTTTTTTTTTTTTT	70°C

Table 2: Name, sequence, (optimized) annealing temperature (T$_A$)

2.2 Cell Culture Methods

2.2.1 Cultivation of Mesenchymal Stem Cells

Rat adipose-derived mesenchymal stem cells are primary cells capable of differentiation towards osteoblasts. Cells were cultured for three passages in Dulbecco`s Modified Eagle Medium high glucose (DMEM, Sigma-Aldrich, Steinheim, Germany) supplemented with 10% (v/v) FCS (PAA, Pasching, Austria), 1% (v/v) antbiotics (Penicillin-/Streptomycin, PAA, Pasching, Austria) and 1% (v/v) glutamine (PAA, Pasching, Austria).

2.2.2 Cell Viability Assay

Cell viability/proliferation was evaluated by MTS assay (Promega, Madison, USA), based on the bioreduction of tetrazolium compound [3-(4,5-dimethylthiazol-2-yl)-5-(3-carboxymethoxyphenyl)- 2-(4-sulfophenyl)-2H-tetrazolium] to coloured formazan by living cells. 50 µl MTS solution was added to the cells in 200 µl culture medium. After one hour of incubation at 37°C, the absorbance of the supernatant at 490 nm was recorded with a 96-well plate reader (POLARstar Omega, BMG LABTECH, Austria) (Data Analysis Software: MARS 2.30 R2).

2.2.3 Transfection with Lipofectamine® 2000

Rat adipose-derived mesenchymal stem cells (passage 3), with a confluence of 80% in T175 cell culture flasks, were transfected with Lipofectamine® 2000 Transfection Reagent (Invitrogen, Germany). For efficient transfection, cells were washed with with DMEM high glucose prior to transfection. 45 µg plasmid-DNA was mixed with 4.5 ml DMEM without serum, 90 µl Lipofectamine® 2000 with 4.5 ml medium without serum. After 5 minutes incubation at room temperature, diluted DNA was gently combined with diluted Lipofectamine® 2000 transfection reagent. Within 20 minutes, the stable complexes were supplemented to the 25 ml DMEM (containing 1% FCS) in the flasks. After 6 hours incubation time, medium was exchanged to culture medium, containing 1% Penicillin/Streptomycin.

2.2.4 Osteogenic Differentiation of Mesenchymal Stem Cells in 2D

pmaxGFP and pVax1-BMP2/7 transfected cells were cultured either in DMEM (control medium) or in osteogenic medium for 30 days. For this purpose, cells were transfected in T175 cell culture flasks, trypsinized 24 hours later for seeding 10^5 cells drop-wise to the middle of a 6-well plate. For verification of transfection efficiencies, control cells were transfected with pmaxGFP. Visualization was performed by fluorescence microscopy [Axio ObserverA1 (Zeiss, Germany)] one day after transfection. Cells were cultured either in control medium or in osteogenic medium, respectively, both containing low levels of serum and glucose. Additionally, for enhancement of osteogenic differentiation, 300 ng/ml rhBMP2 (Wyeth, Madison, USA) was added to the medium. The overall experimental set up in detail was performed as follows:

Conditions for osteogenic differentiation:

pmaxGFP transfected	pVax-BMP2/7 transfected
control medium	control medium
osteogenic medium	osteogenic medium
control medium with rhBMP2 (300 ng/ml)	control medium with rhBMP2 (300 ng/ml)
osteogenic medium with rhBMP2 (300 ng/ml)	osteogenic medium with rhBMP2 (300 ng/ml)

Control medium (500 ml):

DMEM low glucose	480 ml	
FCS	10 ml	2%
L-glutamine	5 ml	1%
P/S	5 ml	1%

Osteogenic medium (500 ml):

DMEM low glucose	450 ml	
FCS	10 ml	2%
L-glutamine	5 ml	1%
P/S	5 ml	1%
Dexamethason	5 µl	10 nM (stock: 1 mM)
Ascorbat-2-phosphat	500 µl	150 µM (stock: 150 mM)
ß-glycerophosphat	5 ml	10 mM (stock: 1 M)

2.2.5   Alizarin-Red Staining:

Osteoblasts produce mineralized matrix mainly consisting of hydroxyapatite crystals. Alizarin Red staining method stains calcium deposits red, indicating active mineral deposition.

After 30 days of differentiation, cells were washed three times with PBS and frozen in 70% ethanol at -20°C for about 2 hours for fixation. After a following washing step with ddH$_2$O, Alizarin Red dye (Lifeline Cell Technology, Walkersville, Maryland, USA) (40 mM, pH 4.2) was supplied to the cells. Cells were exposed ten minutes to the substrate and washed with ddH$_2$O to remove unspecific/unbound Alizarin Red stain prior to photo documentation [Axio Observer.A1 (Zeiss, Germany) (4.0 Software (Zeiss, Germany)].

2.2.6   Quantification of Mineralization

Quantification of Alizarin Red staining was accomplished by dissolving the dye in 0.1 M HCL/0.5% SDS for 30 minutes at RT. Then, the calcium content was examined by absorbance measurement at 425 nm (POLARstar Omega, BMG LABTECH, Austria) (Data Analysis Software: MARS 2.30 R2).

2.2.7   Fibrin Clot Fabrication

Tissuecol™ Kit, containing all used components for fabrication of fibrin clot, was purchased from Baxter AG (Vienna, Austria). The fibrin polymer was prepared by combining MSCs one day after transfection (5x10^6 cells in 3 ml) with 1 ml fibrinogen, followed by loading in eppendorf caps. Immediately after, the solution was combined with 150 µl thrombin to form fibrin gels (300 µl) with final concentrations of 2 IU/ml thrombin 4 and 12.5 mg/ml fibrinogen. After gelation for 1 hour at 37°C, clots containing embedded cells were transferred to 24 well plates and medium was added. Culture medium as well as recombinant human BMP2 (InductOS® Wyeth, Madison, NY, USA) were reconditioned every week. In order to prevent dissolving of the 300 µl clots, aprotinin (1% v/v) was regularly supplied to the medium.

2.3 Biochemical Methods

2.3.1 ELISA

An ELISA kit (R&D Systems, USA) was used for quantification of human bone morphogenetic protein 2 and 7 in cell culture supernatants. As suggested, 100 µl diluted Capture Antibody in 1x PBS was applied per well for coating Nunc Maxisorp 96-well plates overnight. Each well was washed four times with 1x PBS and blocked with Reagent Diluent (1% BSA in 1x PBS) for one hour, followed by a further washing step. Standards for calibration were chosen according to the instructions of the manufacturer (rhBMP2: 0, 47, 94, 188, 375, 750, 1500, 3000 pg/ml; rhBMP7: 0, 62.5, 125, 250, 500, 1000, 2000, 4000 pg/ml). After adding 100 µl sample or standard (diluted in Reagent Diluent) to each well, the plates were covered with an adhesive strive for incubation for 2 hours. Then plates were prepared by washing for a total of four washes and 100 µl diluted detection antibody in Reagent Diluent was applied to each well for incubation for 2 hours. The plates were washed again four times and after the last washing step, remaining Washing Buffer was removed by blotting against clean towel papers. After adding 100 µl Streptavidin-HRP and 100 µl substrate solution followed by a further washing step, 40 µl Stop Solution (1 M H_2SO_4) was applied. Thereby, a caloric change from blue to yellow could be observed in the wells. Determination of substrate reaction was carried out using a microplate reader (POLARstar Omega, BMG LABTECH, Austria) set to 450 nm with a wavelength correction of 540 nm.

3 Results

3.1 Cloning of Osteoinductive Genes

As preparation for future experiments, Wnt5a and Wnt7a cDNA sequences were cloned into pVax1 by the gateway system and sequenced with T7 backbone primer. These sequences were conform with published Wnt5a and Wnt7a sequences. For detailed description of cDNA sequences refer to appendix.

3.2 Comparison of Different Charges of rADSCs

For optimizing transfection conditions, five charges of rADSCs (rADSC 14, 18, 21, 42, 43, which were each pools of ADSCs isolated from fat pads of individual rats) were chosen and transfected with Lipofectamine 2000 transfection reagent. Therefore, two different DNA to Lipofectamine ratios were taken, 1:1 and 1:2. After 24 hours, pictures were taken from the GFP transfected cells to determine transfection efficiency and a cell viability test (MTS-Assay) was performed.

Microscopy and MTS-Assay data confirmed that the charges differ widely in morphology and cell behaviour regarding transfection efficiency (20-40%) and cell viability (figure 16 and 17). Generally, all charges had a higher transfection efficiency with 1 μg DNA and 2 μl Lipofectamine 2000 than with the 1:1 ratio (figure 16). Furthermore the MTS-Assay showed that 2 μl Lipofectamine is barely more toxic than 1 μl, except for the charge rADSC 43, in which a decline of about 50% was observed (figure 17). In total, comparison of transfected cells to controls indicate a decline in viability of approximately 0 (rADSC 42) to 50% (rADSC 43), dependent on Lipofectamine2000 amount and rADSC charge.
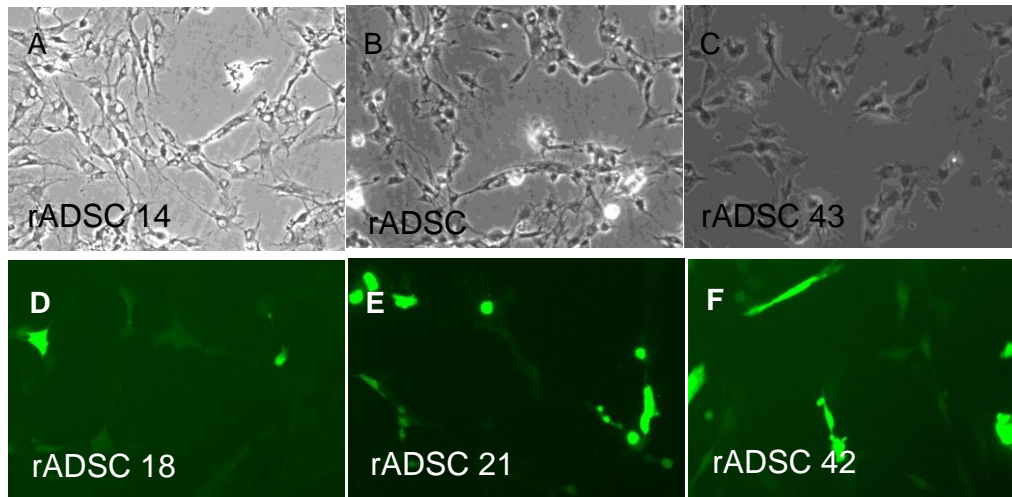
Figure 16: Cell morphology and GFP positive cells. Different cell shapes (A-C) and varying number of green fluorescent cells (D-F) are shown. A: rADSC 14, B: rADSC 18, C: rADSC 43; D: rADSC 18, E: rADSC 21, F: rADSC 42
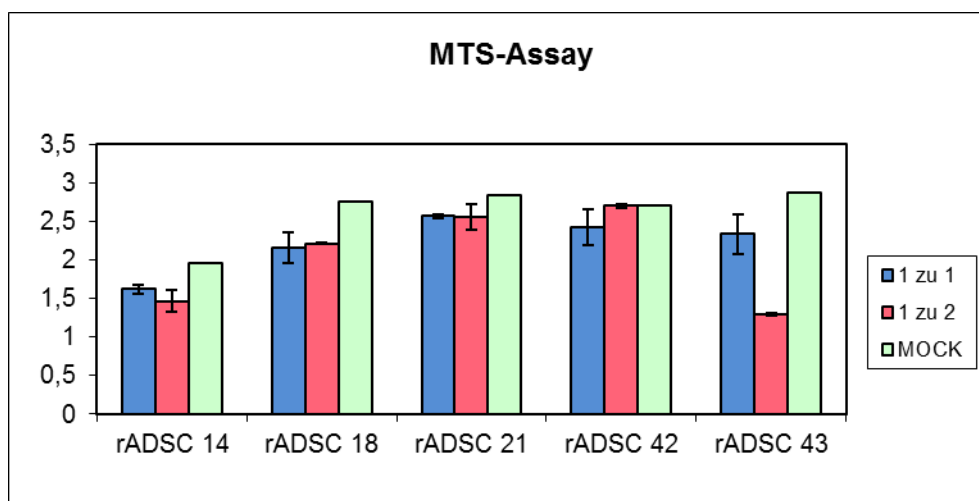

Figure 17: MTS Assay. Diagram illustrating cell viabilities of rADSCs (rADSC 14, rADSC 18, rADSC 21, rADSC 42, rADSC 43) after transfection. MOCK (untransfected cells) were used as references. Data represent mean values (n=2), except of controls (n=1). TR: transfection reagent (Lipofectamine 2000) Data are depicted as mean ± SD of measured OD 492 nm values in the MTS assay.

3.3 Analysis of Transfection Efficiency of pVax-BMP2/7 Compared to pmaxGFP

For comparison of transfection efficiencies, the charge rADSC 11 was chosen and either transfected with pmaxGFP or pVax-BMP2/7. After DNA extraction and plasmid-DNA preparation, concentration quantification was carried out using real-time PCR. By means of standard series, the plasmid concentration/copy number could be determined (figure 18).
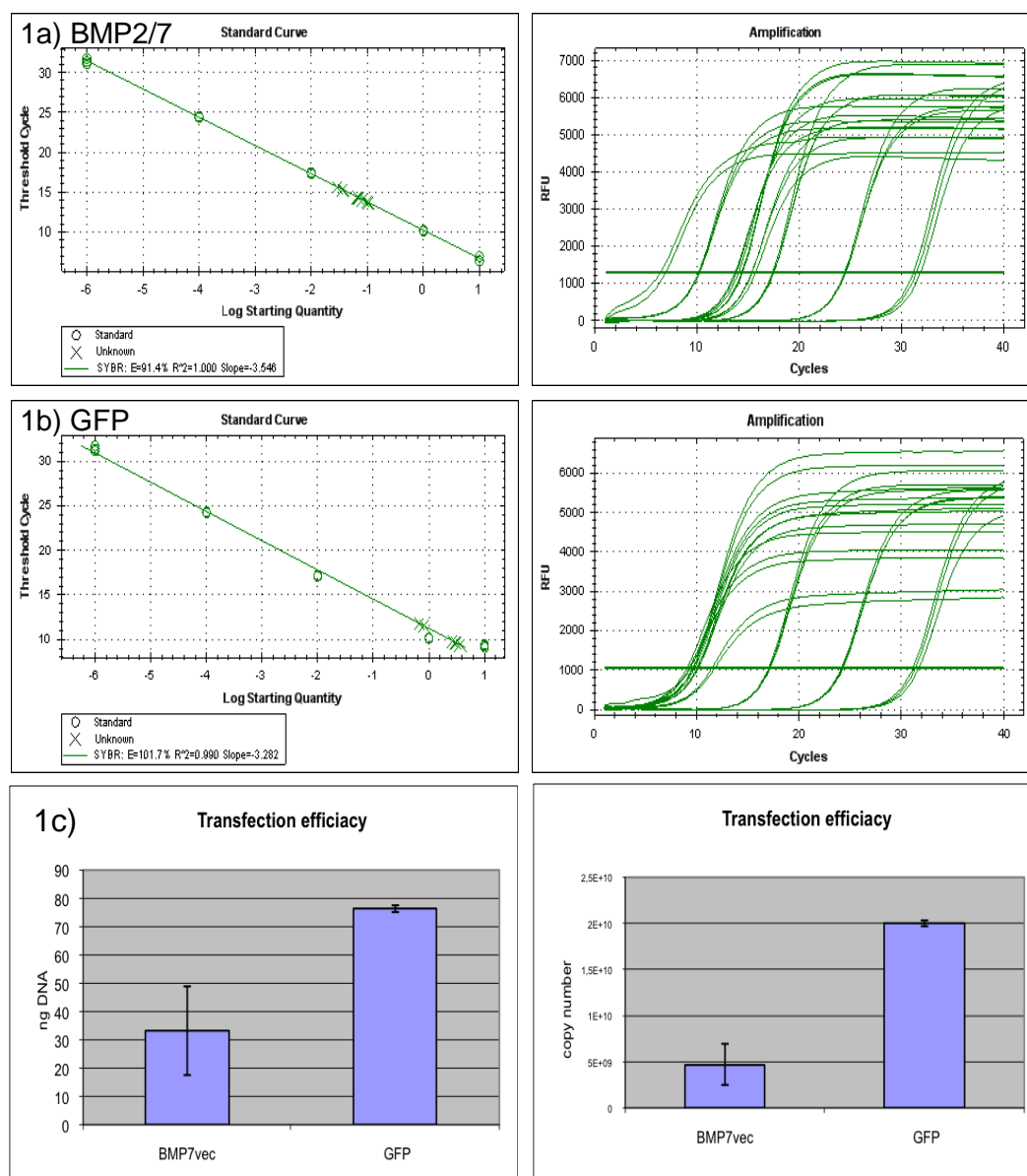

Figure 18: qPCR data. Figure 1a and 1b showing standard curves (linearity of standard values) and treshold cycles of BMP7 and GFP; figure 1c showing comparison of BMP7 amount (specific primer for BMP7-vector DNA) with GFP amount. Furthermore copy number was calculated, based on real-time
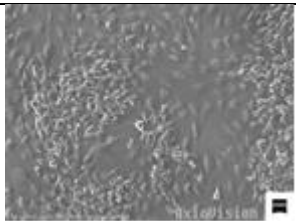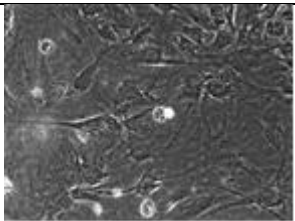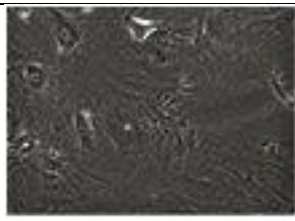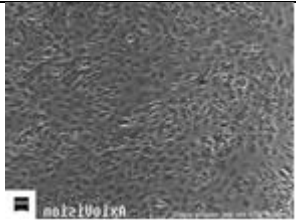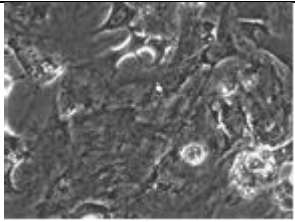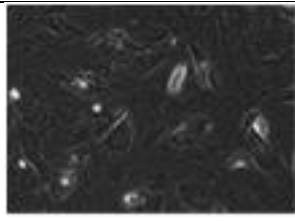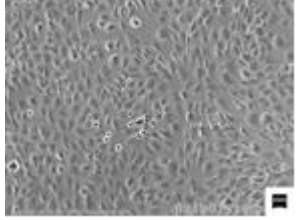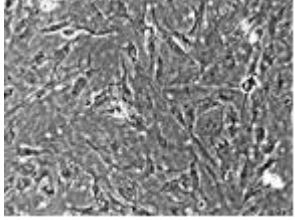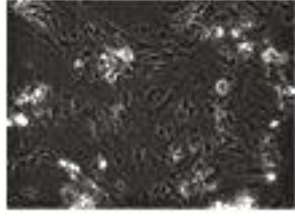
PCR results. Relying on DNA amount results (ng) as well as copy number data, pmaxGFP has definitely higher transfection efficiency as pVax-BMP2/7. Data represent mean values ± SD of n=3.

3.4 Osteogenic Differentiation of Transfected rADSCs in 2D with rhBMP2

In order to evaluate the highest possible stimulus for rADSCs to differentiate to osteoblasts, rhBMP2, pVaxBMP2/7 and osteogenic medium were applied. Besides single application (using a therapeutic gene, therapeutic protein or an osteogenic medium respectively to recruit MSCs towards the osteoblast lineage), combination approaches were performed to enhance osteogenic differentiation. The evaluation of differentiation was based on light microscopy (figure 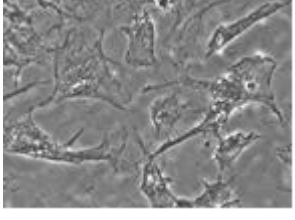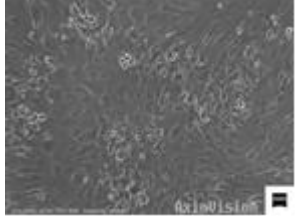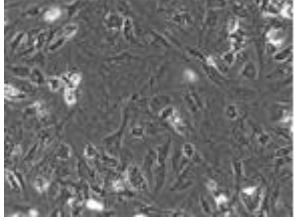19), Alizarin Red staining (figure 20), quantification of mineralization (figure 21), real-time PCR (figure 22) and ELISA (figure 23).

3.4.1 Light Microscopy

Changes in cell number were already observed after 6 days of culture as shown in figure 19. After 16 days all cells (independent of their osteogenic treatment (BMP2/7 transfection, osteogenic medium, 300 ng rhBMP2) illustrated changes in morphology. On day 30, cells illustrated same morphology as already observed on day 16.

		6 days	16 days	30 days
pmaxGFP	control medium			
	osteoinductive medium			
	control medium + 300 ng rhBMP2			
	osteoinductive medium + 300 ng rhBMP2			

		6 days	16 days	30 days
pVax–BMP2/7	control medium			
	osteoinductive medium			
	osteoinductive medium + 300ng rhBMP2			
	osteoinductive medium + 300 ng rhBMP2			
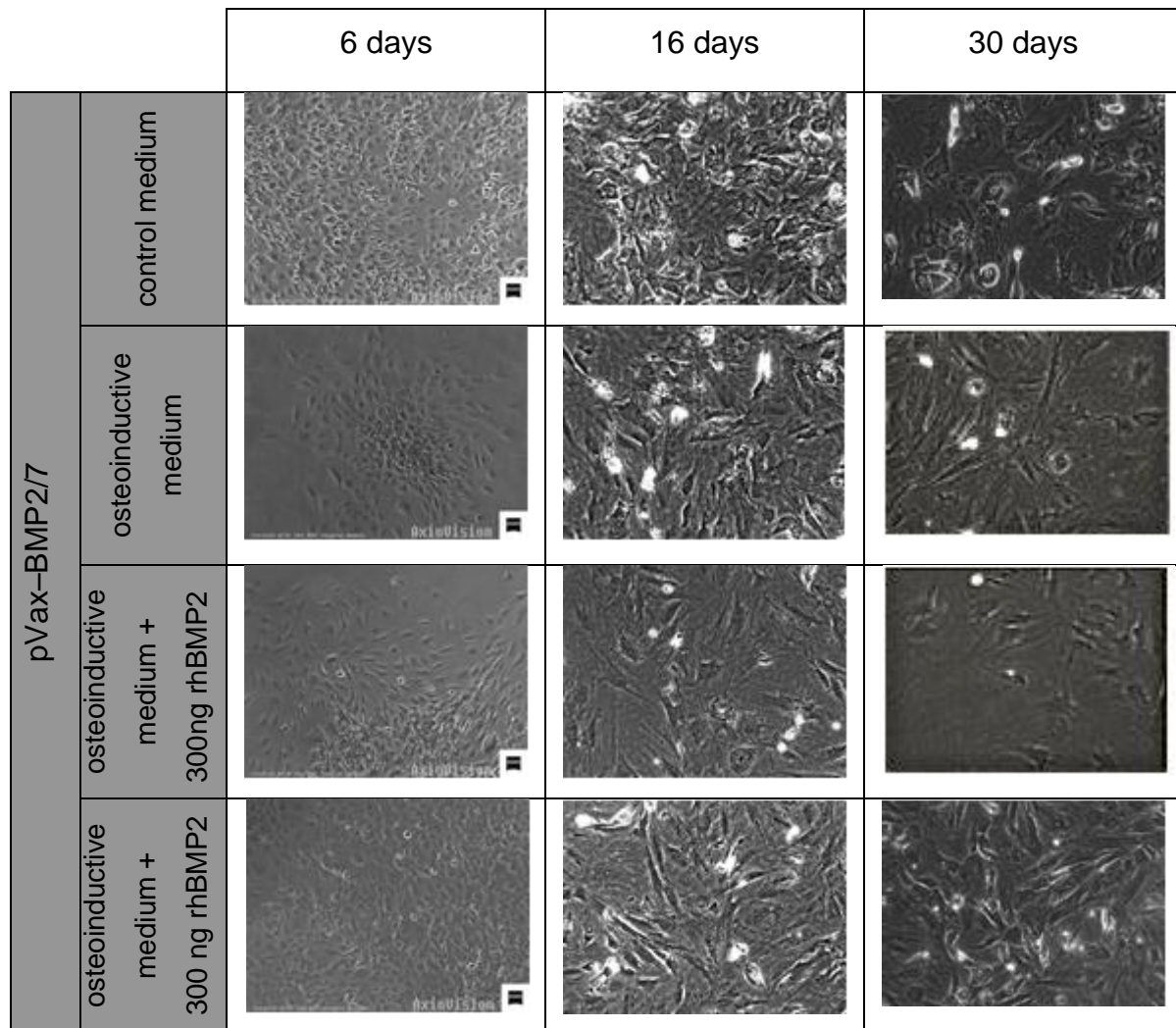
Figure 19: Microscopy of rADSCs after induction of osteogenic differentiation. Time points of this experiment: 6 days, 16 days and 30 days after transfection. On the sixth day, cell density declined in BMP2/7 transfected cells but on day 16, these cells showed a similar cell number as GFP transfected cells.

3.4.2 Alizarin Red Staining

In order to verify osteogenically differentiated cells, Alizarin Red staining was performed, showing positive depositions in all BMP treated cells (figure 20). In general, pictures demonstrate that the presence of osteogenic medium strongly enhances osteogenic differentiation. An especial high calcium deposition has been observed after application of an osteogenic medium combined with 300 ng recombinant human BMP2. The highest calcium precipitates are depicted in figure 20 in D and H.

A-D: pmaxGFP transfected cells

A

Control medium

B

Osteogenic medium

C

Control medium with 300ng rhBMP2

D

Osteogenic medium with 300ng rhBMP2

E-H: pVax-BMP2/7 transfected cells

E

Control medium

F

Osteogenic medium

G

Control medium with 300ng rhBMP2

H

Osteogenic medium with 300ng rhBMP2
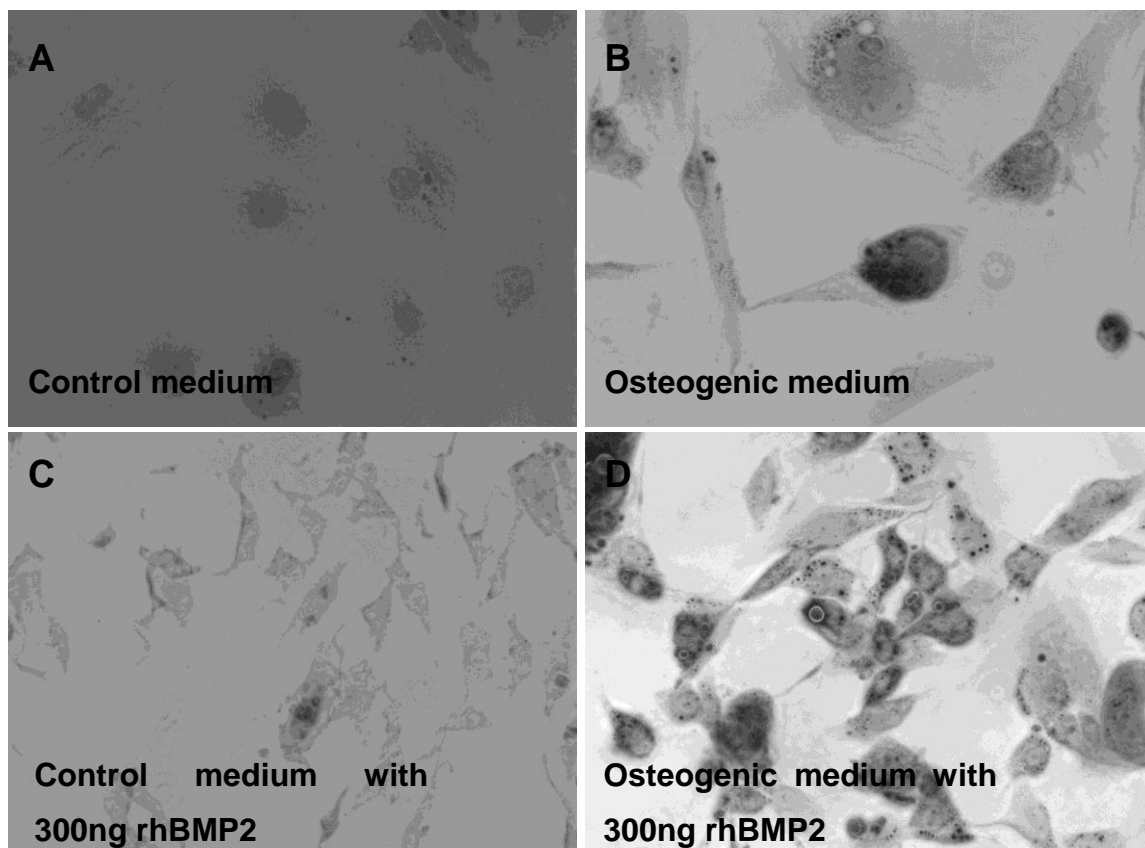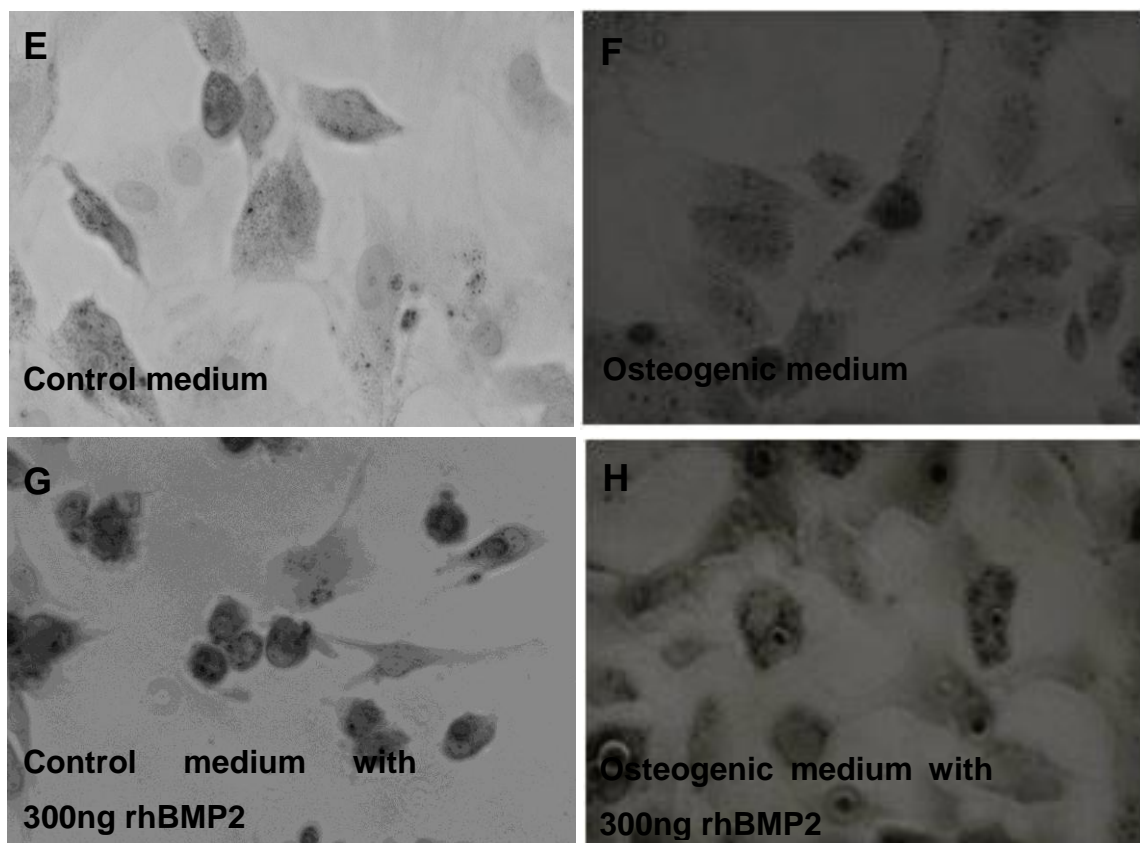
Figure 20: Alizarin Red staining. Accumulation of dots in the cells (red dots, in photographs appearing black; caused by using a black/white camera), (occuring in especially high quantity in D and H) indicate staining for calcium depostitions, a sign of osteogenic differentiation. A-D illustrate GFP transfected cells, E-H BMP2/7 transfected cells.

3.4.3   Calcium-Measurement

For quantification of calcium deposits (index for mineralized matrix/cell), cells were washed with PBS a few times, removing excessive stain residuals in the wells from the pre-performed Alizarin-Red staining. Unfortunately, thereby calcium was removed to some extent resulting in very similar data for all samples in calcium measurement, giving a complete different (meaningless) result compared to PCR, morphology and staining data.
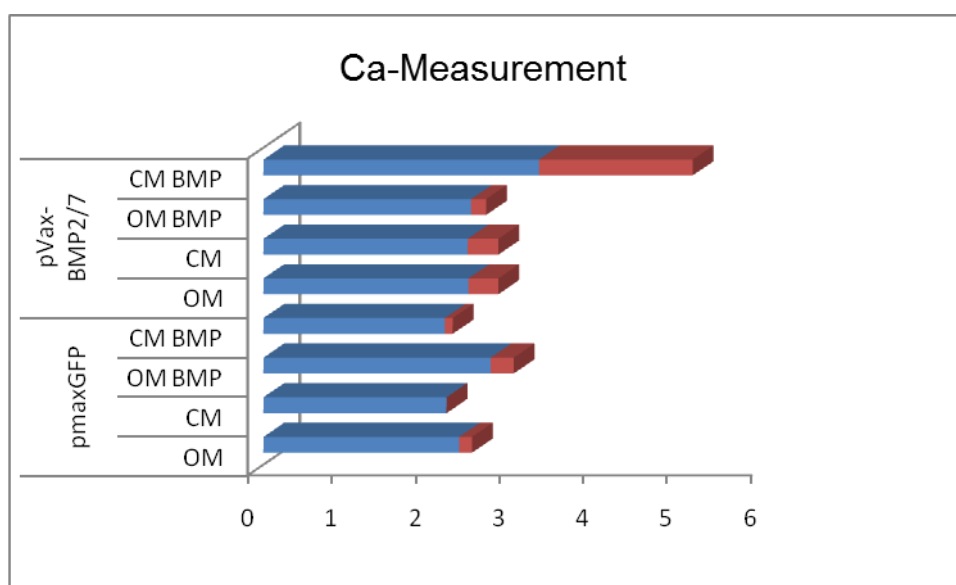
Figure 21: Ca-Measurement. Blue bars correspond to quantified calcium values and represent mean values of n=3. Red bars index SD.

3.4.4   qPCR

Quantitative real-time PCR was used, confirming morphology and alizarin red staining results. In GFP and BMP2/7 positive cells, cultured in conventional DMEM for four weeks, no osteocalcin and no sialophosphoprotein-1 expression could be detected thus assumable that no osteogenic differentiation has taken place (figure 22). Furthermore, it could be observed (illustrated in the graphs in figure 22) that pVax-BMP2/7 transfection had only an impact on osteocalcin expression, if 300 ng rhBMP2 was added to the medium. Regarding ALP expression, pVax-BMP2/7 is to some extent effective without the addition of any other substances.
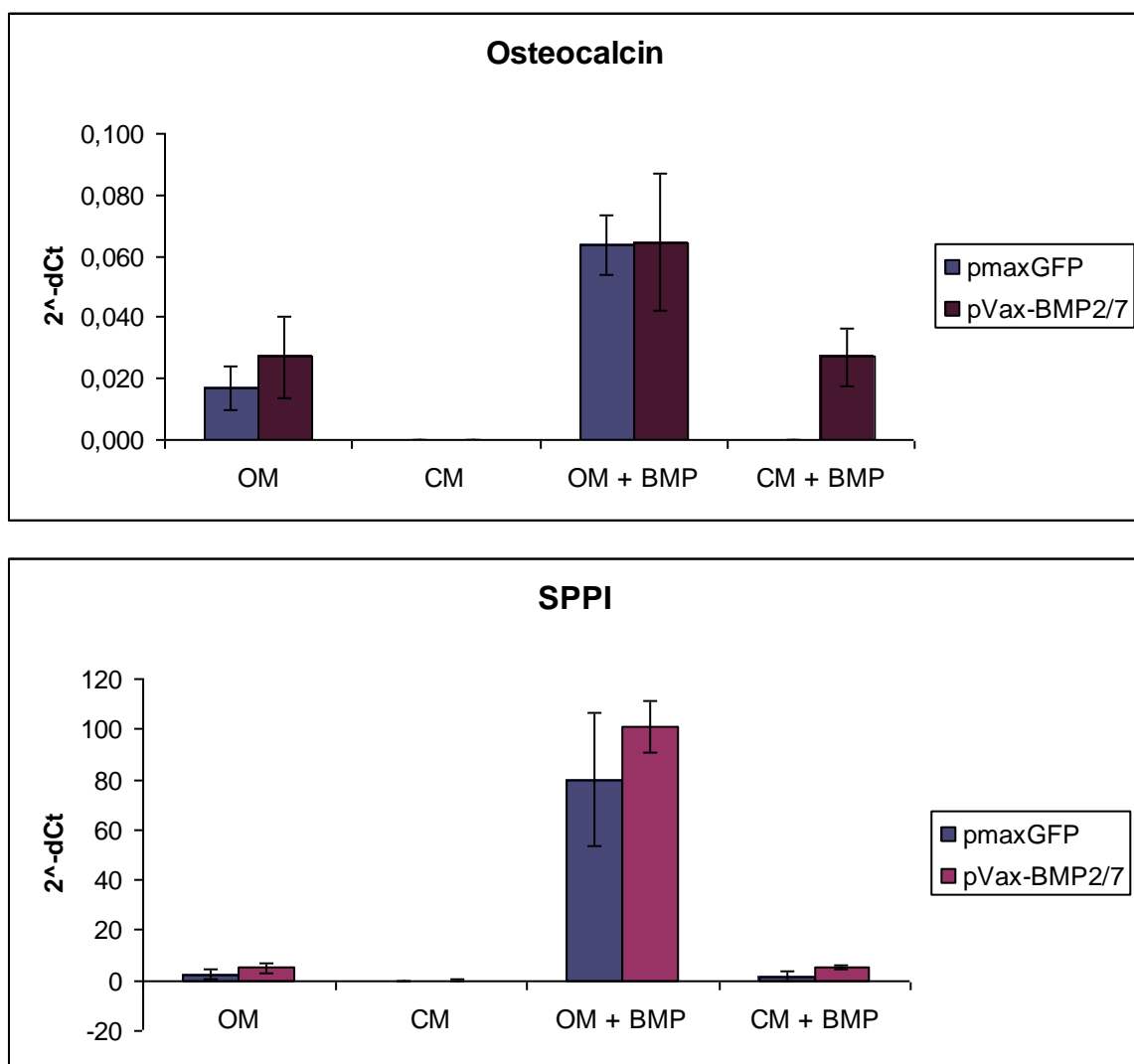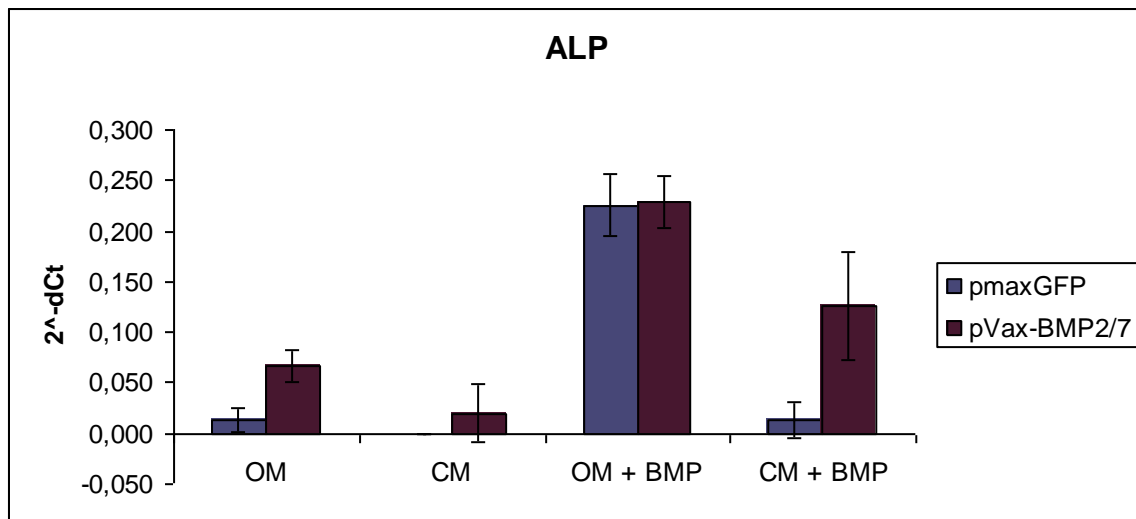
Figure 22: Osteocalcin (OC), sialophosphoprotein I (SPPI) and alkaline phosphatase (ALP) expression at mRNA level as determined by qPCR. Relative expression data were calculated with the use of HPRT as reference control. Legend indicating plasmids used in transfection approach. OM: osteogenic medium, CM: control medium, OM + BMP: osteogenic medium with 300 ng rhBMP2, CM + BMP: control medium with 300 ng rhBMP2. Data represent mean values of n=3 ± SD.

3.4.5   ELISA

For quantification of the protein level of BMP2 in the supernatants of rADSC 42, an ELISA was performed. BMP2 protein expression is about 6 fold higher in induced cells compared to controls (cells in culture medium) on day 14 and day 20.
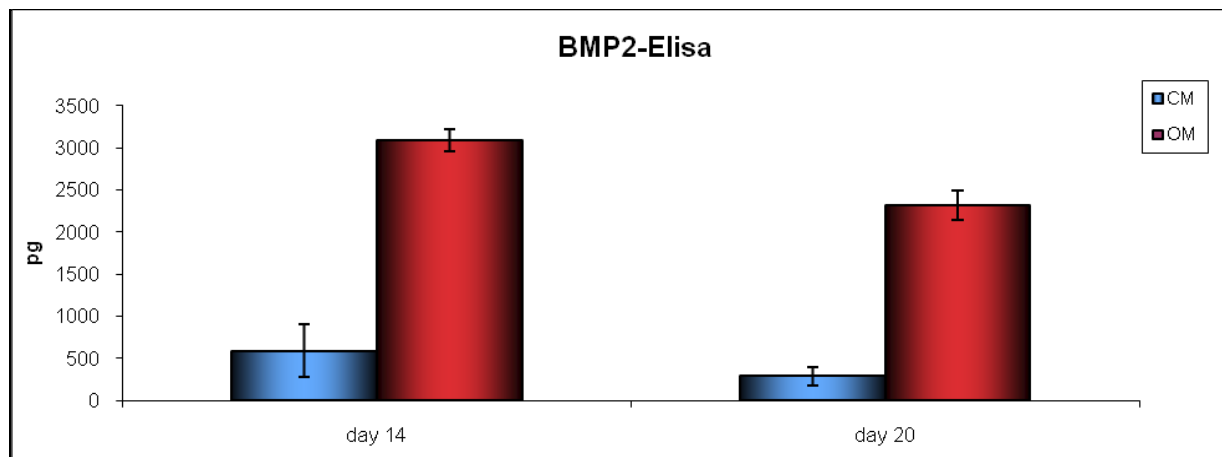
Figure 23: BMP2-ELISA, BMP2 protein expression of induced cells (osteogenic medium, n = 2 ± SD) in contrast to controls (control medium, mean of n = 3 ± SD), 14 days and 20 days post-transfection. CM = control medium, OM = osteogenic medium

3.5 Osteogenic Differentiation of Transfected rADSCs in 3D with rhBMP2

Due to the fact, that 2D cell conditions are affecting seeded cells differently compared to 3D environment, fibrin gels with included rADSCs were generated. In addition, the 3D clots resemble more the *in vivo* physiology for instance regarding cell-matrix interaction, nutrition and waste transport. GFP positive cells enabled observation of cell distribution within the matrix and proliferation/amount in the biomaterial over time. Thereby, uniformly distributed cells, as well as cell divisions could be observed under the microscope (data not shown since no sufficiently sharp photo documentation of the GFP positive cells was possible in 3D, due to the different planes inside the fibrin clots). During the experiment, aprotinin (1% v/v) was regularly applied to the medium to prevent dissolution of the fibrin clot. Medium was changed every week and 300 ng

rhBMP2 added. At the same time, aliquots were frozen at -80°C for subsequent ELISA analysis.

3.5.1　Light Microscopy

The fibrin clot morphologies and sizes were influenced by the different conditions. The resulting variation in clot densities (illustrated in figure 24) may be caused by alterations in the extracellular matrix generated by contained cells. It is obvious that the presence of bone morphogenetic proteins and culture medium determine clot characteristics/attitude.

pmaxGFP transfected cells:

CM　　　　**OM**　　　　**CM + rhBMP2**　　　　**OM + rhBMP2**

pVax-BMP2/7 transfected cells:

CM　　　　**OM**　　　　**CM + rhBMP2**　　　　**OM + rhBMP2**

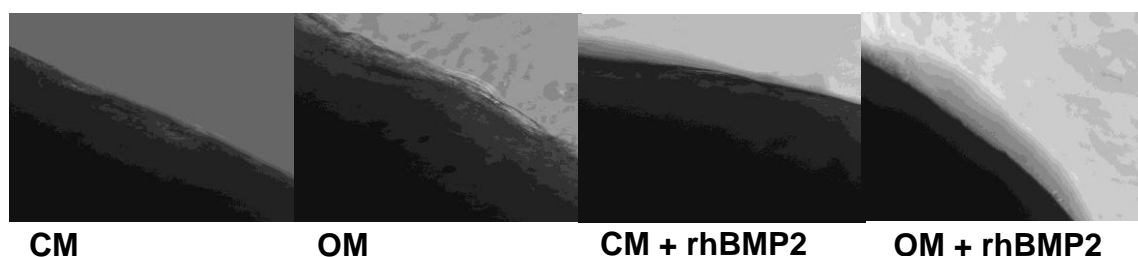Figure 24: Microscopy of fibrin borders after 30 days of culturing (end of the experiment). Especially dense (black) and clearly drawn borders are depicted in cells treated with an osteogenic medium and rhBMP2.

3.5.2   qPCR

Quantitative real-time PCR was performed, confirming morphology results. In GFP and BMP2/7 positive cells cultured in conventional DMEM for four weeks, no osteocalcin and no sialophosphoprotein 1 expression could be detected, thus assumably no osteogenic differentiation has taken place. Furthermore, it can be observed in figure 25, that pVax-BMP2/7 has no impact on osteocalcin expression. Due to this unexpected result, the plasmid was analysed by various restriction digestions. One out of three separate restriction reactions revealed a wrong band pattern. Unfortunately, the control digestion, which was performed to check the plasmid before the main experiment was started, produced band patterns that indicate successful generation of the desired construct. Presumably, some unwanted recombination processes occurred during plasmid amplification. Therefore, expression levels of osteogenic genes were only determined for the GFP transfected cells (figure 25). qPCR data show, that an osteogenic medium with 300 ng rhBMP2 highly upregulates osteocalcin expression. Moreover, an inductive potential of rhBMP2 was determined in ALP expression and also in slight tendency in SPPI expression. No differences among the 4 different osteogenic approaches could be observed regarding collagen type I expression.

SPPI

ALP
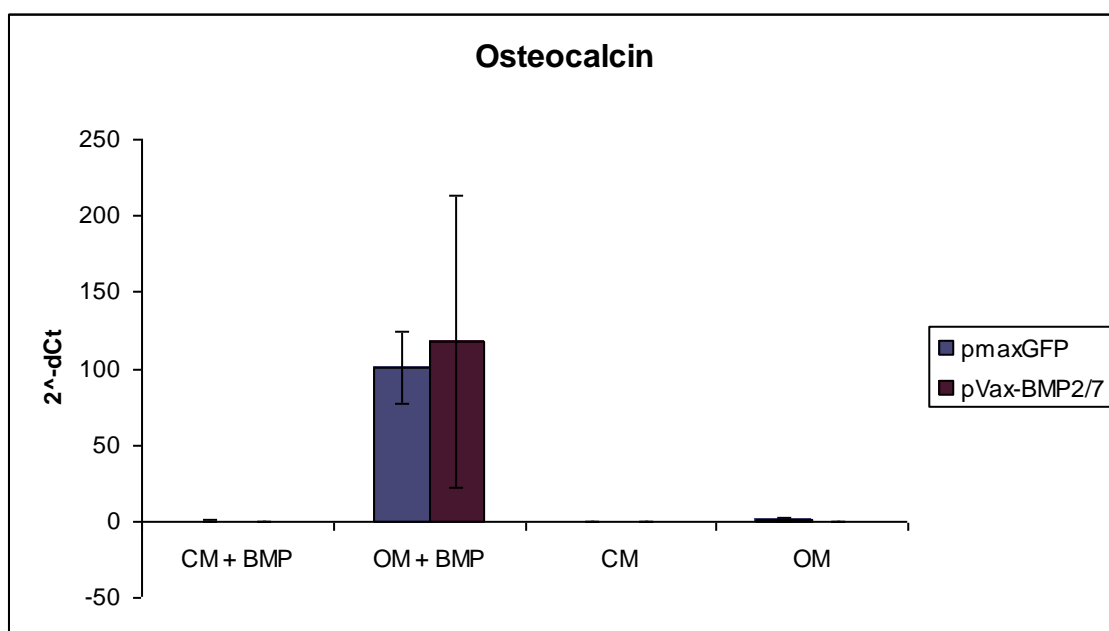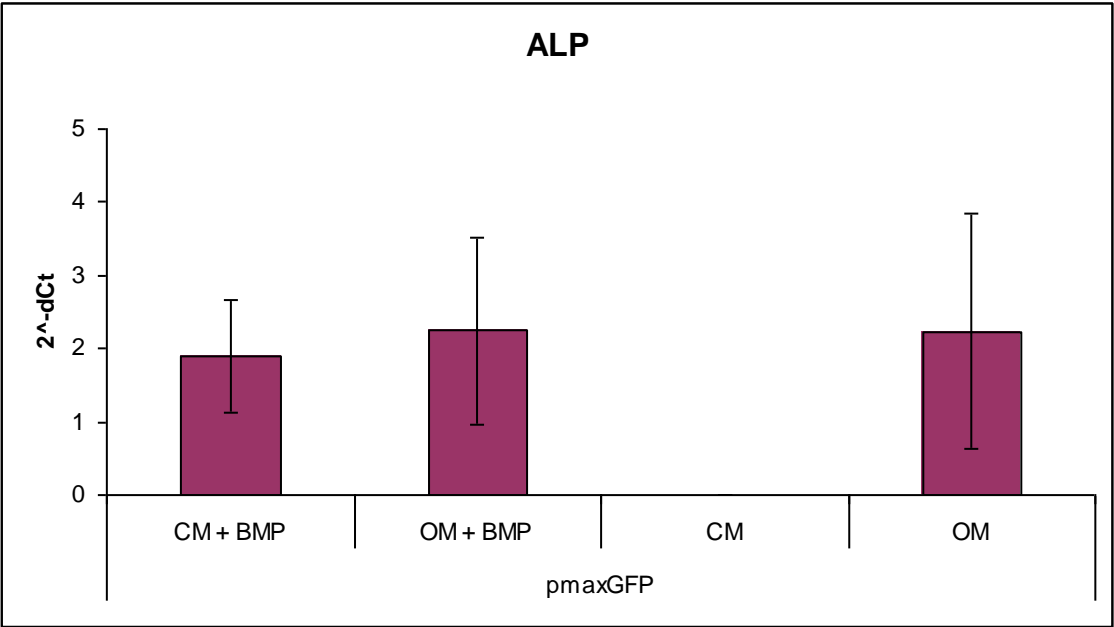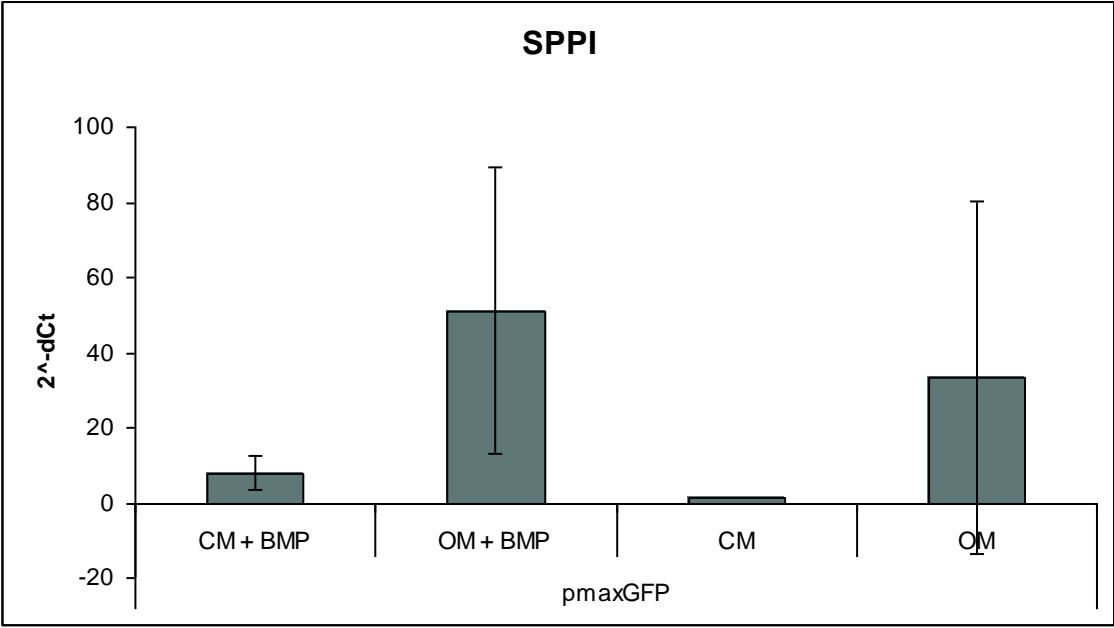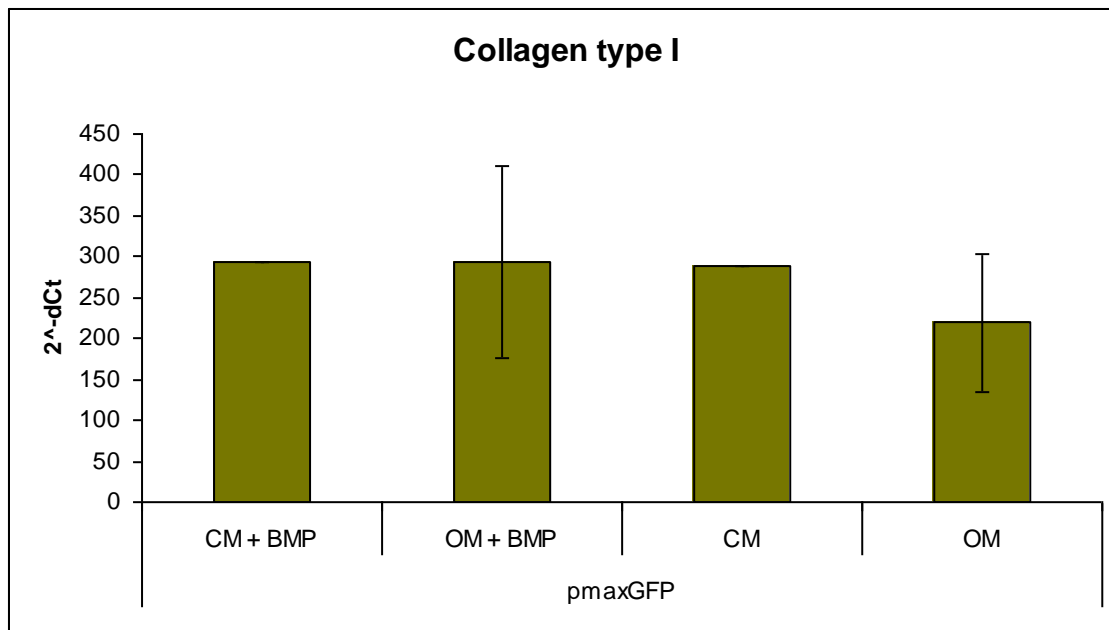
Collagen type I

Figure 25: Osteocalcin (OC), sialophosphoprotein I (SPPI), alkaline phosphatase (ALP) and collagen type I expression (Col1) in fold change relative to reference control (HPRT) after 30 days of differentiation. Control cells treated with DMEM (CM), cells induced with osteoinductive medium (OM), cells induced with 300 ng rhBMP2 in DMEM (CM + BMP), cells induced with 300 ng rhBMP2 in osteoinductive medium (OM + BMP). Almost all data represent mean values of n=3. By reason of limited amount of cDNA, collagen expression depicts mean values of n=2 (CM: n=1). Mean ± standard error of the mean (mean ± SEM).

4 Discussion

4.1 Comparison of Different Charges of rADSCs

Adipose tissue-derived stem cells (rADSCs), a type of adult stem cells, can be easily isolated from the human body to be used for tissue regeneration. Past reports demonstrated multipotency of these cells with the ability to differentiate into chondrocytes, osteocytes and adipocytes [68], which gave rise to great interest in biomedicine. According to literature, MSCs are very sensitive, so that isolation, expansion and culture protocols highly affect their cell properties such as proliferation and differentiation potential [69]. The isolated fat (by liposuction) contains a multitude of cells including haematopoietic-lineage cells, endothelial cells or pericytes, so variable isolation and culture conditions favor expansion of certain cell types at the expense of the others [70], [71]. Also, the cell composition of the patients might be variable affecting the rate of success, which make them to difficult tools for clinical translation. Moreover, it has been demonstrated that aged human mesenchymal stem cells show a lower differentiation and proliferation potential [72]. According to these findings, within this study, we first aimed at the comparison of adipose-derived stem cells – in this case pooled charges isolated from different rats - and to evaluate the most efficient MSCs regarding their stem cell character for the following experiments. Indeed, great differences were detected in cell morphology and transfection efficiency (ranging between 20-40% with Lipofectamine 2000 transfection reagent) among the 5 different rADSC charges. A MTS Assay 24 hours post-transfection revealed, that one out of five charges showed a decrease (of 50%) in cell viability when using double amount of Lipofectamine. Moreover, the comparison of cell numbers after transfection to controls showed a decline between 8 up to 50% between the different charges, indicating variable sensitivity to the tranfection conditions. By reason of these findings, it can be concluded that the mesenchymal stem cells isolated from different animals/individuals differed widely in their features. Probably, the variability of age and health status among the animals as well as the differences in handling/isolation by two individual persons can be responsible for these results. Therefore, we conclude that an establishment of standardized protocols and a detailed definition (surface marker characterisation) of

MSCs is necessary for beneficial clinical application in the future [68].

4.2 Transfection Efficiencies

For tissue regeneration, non-viral vectors are considered to be most likely a suitable candidate for clinical translation. Plasmids do not integrate in the genome in contrast to viral vectors, which is a crucial factor for safe and transient therapy [73]. Furthermore the higher bioactivity of endogenously synthesized proteins, which may be explained by host specific post-translational modifications, should make them to a successful and cost-effective application. Moreover, gene therapy has already demonstrated to be effective *in vivo* for instance in wound healing [74] and muscoskeletal regeneration. Unfortunately, low transfection efficiencies (when not accompanied by adjuvants) limit these multiple beneficial features [75]. Since DNA uptake, especially by cationic lipid-mediated gene transfer is dependent on many parameters like pH, structure and size of lipoplexes, in the present study the transfection efficiencies of different gene constructs were compared *in vitro*. Therefore pmaxGFP and pVax-BMP2/7 were introduced into cells and the internalized plasmid DNA was isolated for highly sensitive detection by qPCR. Interestingly, highly variable DNA amounts were obtained. A possible explanation for this result could be a variable strength of electrostatic interactions between positive charge of liposome/DNA complexes to the cell surface, as this has been suggested to be a highly influential factor [76], [77].

According to the results it can also be concluded that a separate positive control reporter is not suited to verify successful transfection reactions of a therapeutic gene. For this reason, co-delivery of therapeutic and control gene via a single plasmid (bicistronic vector) should be an advantageous/possible option.

4.3 Osteogenic Differentiation

Gene therapy has been developed to be one of the most promising approaches for successful clinical translation in the future. In the last years there has been a big optimism for the success of recombinant BMPs for bone regeneration. Over one million people have already been treated for spinal fusion, non-union fractures, craniomaxillofacial and periodontal bone defects with BMP2 or BMP7 [13]. Unfortunately, the results obtained from the clinics demonstrated quite often problems in protein stability [34] and limitations in osteogenic activity. This is may be caused by an up-regulation of signaling antagonists. In a present study, the administration of high amounts of recombinant bone morphogenetic proteins (which are needed to be effective) dramatically raised expression level of Noggin [33]. In another study, this growth factor stimulated the generation of osteoblasts, but also the number of osteoclasts increased at the injury site mediated through RANKL/Osteoprotegerin [78]. By reason of these findings and due to the high production costs, routine application of recombinant proteins won't be worthwhile.

The aim of this study was to show that a gene therapeutic approach could enhance processes involved in bone formation in vitro. It has been shown that combinatorial expression of therapeutic genes such as BMP subtypes with angiogenic factors or with the osteogenic transcription factor Runx2 could induce new bone formation to a higher quality and quantity *in vitro* and *in vivo* [27], [79]–[82]. As demonstrated, gene transfer of BMP2/7 heterodimer has a higher bone formation activity than application of BMP2 or BMP7 alone [80], [82]. Indeed, within this study the co-transfection of rADSCs with the heterogenic growth factor BMP2/7 via a single plasmid showed increased expression levels of osteogenic markers such as alkaline phosphatase, osteocalcin, and sialophosphoprotein 1. A calcium specific staining (Alizarin red) confirmed the high bioactivity of this growth factor in mineral matrix formation. Moreover, an increase of this co-expression strategy for osteogenic induction could be observed with a conditioned medium composed of dexamethasone, ascorbat-2-phosphate and ß-glycerolphosphate as recommended for mesenchymal stem cells in many studies [83]–[85]. This medium has been reported to induce especially high bone formation in combinatorial therapies with recombinant BMP2 in MSCs of rats [86]. A possible explanation for these finding has been demonstrated in a previous study, where a change in the phosphorylation state of osteogenic transcription factor

Runx2 has been detected in cells cultured in an osteogenic medium [87]. Interestingly, control cells cultured in an osteogenic medium with 300 ng rhBMP2 obtained similar expression levels of osteogenic genes as BMP2/7 treated cells, which were cultured in the same conditions. Out of this data, it can be suggested that BMP2/7 has a high osteoinductive potential in a conventional culture medium (ten times higher expression of SPP in BMP2/7 transfected cell compared to GFP transfected cells). However, the effect of the plasmid is no more visible if an osteogenic medium or recombinant BMP2 is additionally used.

Furthermore the impact of recombinant growth factors and of an osteogenic medium was investigated in 3D. According to tissue engineering approaches, bone formation can be enhanced with a carrier material [7]. It can fill the gap and can facilitate production of extracellular matrix. Moreover a biomaterial can be loaded with cells, growth factors or genes to accelerate healing [64].

Thus, natural occurring fibrin was used, a biomaterial providing optimal conditions for invading cells [88], [89]. For instance, it contains extracellular matrix proteins like fibronectin and growth factors (VEGF, TGF-ß, FGF, EGF), which are involved in cell recognition, adhesion and angiogenesis [63]. To follow and understand cell behaviour in the clots (in the 4 weeks lasting differentiation experiment), GFP positive cells were introduced. These cells were not only uniformly distributed; they also demonstrated cell divisions in all planes. Moreover, hardly any cells were found to have migrated outside of the biomaterial, indicating that fibrin is a suitable scaffold for cell habitation. Dependent on cell conditions (medium, therapeutic protein, therapeutic genes), different densities of the fibrin matrix, as visualized by light microscopy of clot borders, were detected at the end of the experiment. Presumably, this fibrin clot characteristic is associated with the level of cellular alterations associated with differentiation. Cells that have increased in number and differentiated towards osteoblasts may have increased the production of extracellular matrix, which is mainly constituted of collagen type I, for subsequent deposition of minerals. Possibly, as a result, the biomaterial got retracted from the formed collagen fibres leading to a decrease in size and in increase in clot density. For a more detailed analysis of the events, possibly connected to these observations by light microscopy, real-time PCR was performed. However, no differences in collagen type I expression could be observed in presence or absence of an osteogenic medium or rhBMP2. In contrast, varying expression levels of alkaline phosphatase and sialophosphoprotein

1 were detected when comparing the different differentiation approaches. A high ALP expression was achieved if cells were treated with rhBMP2 and/or cultured in an osteogenic medium. As ALP is an early differentiation marker (necessary for depositions of minerals on the pre-synthesized matrix), cells treated with a conventional medium may not have reached this differentiation status. Probably, these collagen producing cells where on the initial way of differentiation and were right before the onset of ALP expression. Quantification of sialophosphoprotein 1 by qPCR revealed that an osteogenic medium is more effective to differentiate MSCs towards osteoblasts than the usage of rhBMP2. Moreover combinatorial application of these two factors enhanced the expression of this marker. Further, it was shown that also highest osteocalcin levels were achieved by the presence of an osteogenic medium combined with 300 ng rhBMP2. The expression level was about 100 times higher compared to cells treated with an osteogenic medium alone. According to this data, the MSCs may express the following markers in the denoted range towards osteogenic differentiation *in vitro*:

Alkaline Phosphatase → Sialophosphoprotein 1 → Osteocalcin. Therefore it may be of advantage to analyse in detail the differentiation status in the different osteogenic approaches.

Direct comparison of 2D data with 3D data using qPCR demonstrated a supportive feature of a biomaterial in osteogenesis. In all differentiation approaches, ALP was highly up regulated (10-100x), SPP also showed increased levels, but to a minor extent (5-10x) and OC (40-100x) was also highly increased (40x) in 3D when compared to 2D results. In general, results demonstrate the high impact of an osteogenic medium and rhBMP2 alone or in combination. The highest degree of differentiation was achieved by application the combination of fibrin, the osteogenic medium and 300 ng rhBMP2. Although all targets where highly up-regulated in this combinatorial approach, osteocalcin expression was especially high in comparison to 2D data showing a tremendous up-regulation of 1500-fold. Possibly, the characteristics of the biomaterial fibrin are the reason for this tremendous increase but also the 3D structure alone, which builds up the basement for subsequent bone development, can be responsible for this strong induction of osteocalcin level. In order to reveal the original cause of this result, further experiments will have to be performed. This could include the cultivation of rADSCs on a thin layer of fibrin in 2D, to observe the influence of fibrin by itself or repeating the same experiment with other

biomaterials such as agarose or collagen to analyse the impact of a 3D structure on osteogenic differentiation.

In this study, we showed that fibrin is a suitable biomaterial to support osteogenic differentiation *in vitro*. It has already been described several times in literature that BMP2/7 co-expression was highly effective in bone regeneration [27], [34], [90]. Unfortunately, the evaluation of the osteogenic potential of BMP2/7 in fibrin could not be conducted in this study. During plasmid preparation, it has probably come to unwanted recombination events during expansion of the positive clone, which was selected by colony PCR. Therefore the obtained "BMP2/7" data set for osteogenic markers of the 4 weeks lasting differentiation experiment remained at similar levels as the GFP data in real-time PCR. As a solution for this problem, SURE (stop unwanted recombination events) cells could be used for amplification of plasmid DNA in the future.

The results obtained in this study provide further evidence for the high inductive potential of recombinant BMP2. Furthermore, the application of an adjusted osteoinductive medium was proven to be effective in promoting osteogenic differentiation in rat adipose-derived stem cells. It has been shown that BMP2 increases nuclear ß-catenin level in pre-osteoblast cells, an essential component of canonical Wnt signalling and the expression of several Wnt genes such as Wnt15, Wnt3a, Wnt7, Wnt5b), hence an interconnection between BMP and Wnt signalling is suggested. Therefore, an enhanced osteogenic differentiation potential could be possibly achieved by co-expression studies of BMP (BMP2, BMP7) with Wnt (Wnt5a, Wnt7a) genes. Wnt5a and Wnt7a switch on the non-canonical (ß-catenin independent) Wnt signalling pathway, which enhances osteogenesis. While Wnt5a increases ALP, osteocalcin and Runx2 expression, Wnt7a suppresses chondrogenic differentiation (favouring bone formation) [91], [92].

We conclude from our in vitro finding that the application of a scaffold soaked in an osteogenic medium is suitable to differentiate MSCs to the osteogenic lineage. Moreover this indicates that it may be suitable to treat MSCs isolated from the patients with therapeutic genes prior to loading into a biomaterial where it can act as factory to synthesize a gene product.

5 List of Abbreviations

A	adenine
ALP	alkaline phosphatase
AMV-RT	avian myeloblastosis virus reverse transcriptase
As	antisense
ATF4	activating transcription factor 4
BMP	bone morphogenetic protein
BMPR-I	BMP receptor I
BMPR-2	BMP receptor II
bp	base pairs
BSA	bovine serum albumin
BPB	bromphenol blue
C	cytosine
CCD	charge-coupled device
cDNA	complementary DNA
CHO	chinese hamster ovary
CMV	cytomegalovirus
dH$_2$O	distilled water
Dlx5	distal –less homeobox 5
DMEM	Dulbecco's modified eagle medium
DMSO	dimethylsulfoxide
DNA	deoxyribonucleic acid
dNTP	2'deoxynucleoside-5'-triphosphate
E.coli	Escherichia coli
ECM	extracellular matrix
ELISA	Enzyme –linked immunosorbent assay
FCS	fetal calf serum
fbg	fibrinogen
GFP	green fluorescent protein
h	hour
IGF	insulin-like growth factor
kb	kilo base pairs
kD	kilo Dalton

LB-medium	Luria broth medium
M	molar
MAPK	mitogen activated protein kinase
M-CSF	macrophage stimulating factor
MCS	multiple cloning site
Mg	milli gram
mM	milli molar
mRNA	messenger ribonucleic acid
MSC	mesenchymal stem cell
NFkB	nuclear factor kB
µg	micro gram
µl	micro liter
ng	nano gram
nm	nano meter
OD_{600}	optical density at 600nm
OC	osteocalcin
OPG	osteoprotegerin
Osx	osterix
P	phosphorylation
PBS	phosphate buffered saline
PCR	polymerase chain reaction
PDGF	platelet-derived growth factor
PGA	polyglycolic acid
PLA	polylactic acid
PTH	parathyroid hormone
pH	potenia Hydrogenii
pmol	pico mol
RANK	receptor activator of nuclear factor-kB
RANKL	receptor activator of nuclear factor-kB ligand
RGD	arginine-glutamine-aspartic acid sequence
rpm	rounds per minute
RT	room temperature
Runx2	runt related transcription factor 2
s	sense

SB	sodium borat
SBE	smad binding elements
SD	standard deviation
sec	second
SMAD	mothers against decapentaplegic and *Sma* derived
Sost	sclerostin
Sox	SRY related high mobility group box
SPP	sialophosphoprotein
STD	standard deviation
T	thymine
T_a	annealing temperature
TGFb	tumor growth factor b
Ub	ubiquitination
U	unit
V	voltage
VEGF	vascular endothelial derived growth factor
Wnt	derived from drosophila wingless, *wg* and from vertebrate *int* genes
XCFF	xylene cyanol FF

6 List of Figures and Tables

7 References

[1] P. Ducy, T. Schinke, and G. Karsenty, "The osteoblast: a sophisticated fibroblast under central surveillance," *Science*, vol. 289, no. 5484, pp. 1501–1504, Sep. 2000.

[2] *Principles of bone biology*, 3rd ed. San Diego, Calif: Academic Press/Elsevier, 2008.

[3] "700.000 Menschen sind in Österreich von der Knochenbruch-Krankheit Osteoporose betroffen," *Presseaussendung*, 2010.

[4] E. Tsiridis, N. Upadhyay, and P. Giannoudis, "Molecular aspects of fracture healing: which are the important molecules?," *Injury*, vol. 38 Suppl 1, pp. S11–25, Mar. 2007.

[5] T. A. Einhorn, "Enhancement of fracture-healing," *J Bone Joint Surg Am*, vol. 77, no. 6, pp. 940–956, Jun. 1995.

[6] van Blitterswijk Clemens, *Tissue engineering*. Elsevier, 2008.

[7] O. P. Gautschi, S. P. Frey, and R. Zellweger, "BONE MORPHOGENETIC PROTEINS IN CLINICAL APPLICATIONS," *ANZ Journal of Surgery*, vol. 77, no. 8, pp. 626–631, Aug. 2007.

[8] P. Sun, J. Wang, Y. Zheng, Y. Fan, and Z. Gu, "BMP2/7 heterodimer is a stronger inducer of bone regeneration in peri-implant bone defects model than BMP2 or BMP7 homodimer," *Dent Mater J*, vol. 31, no. 2, pp. 239–248, 2012.

[9] T. J. Blokhuis, "Formulations and delivery vehicles for bone morphogenetic proteins: latest advances and future directions," *Injury*, vol. 40 Suppl 3, pp. S8–11, Dec. 2009.

[10] R. Lüllmann-Rauch, *Taschenlehrbuch Histologie 10 Tabellen*. Stuttgart; New York, NY: Thieme, 2009.

[11] K. E. Kadler, C. Baldock, J. Bella, and R. P. Boot-Handford, "Collagens at a glance," *J. Cell. Sci.*, vol. 120, no. Pt 12, pp. 1955–1958, Jun. 2007.

[12] M. Gratzl, Ed., *Histologie*, 5.Auflage ed. Springer.

[13] G. Chen, "TGF-β and BMP Signaling in Osteoblast Differentiation and Bone Formation," *International Journal of Biological Sciences*, vol. 8, no. 2, pp. 272–288, 2012.

[14] A. J. Celeste, J. A. Iannazzi, R. C. Taylor, R. M. Hewick, V. Rosen, E. A. Wang, and J. M. Wozney, "Identification of transforming growth factor beta family members present in bone-inductive protein purified from bovine bone," *Proc. Natl. Acad. Sci. U.S.A.*, vol. 87, no. 24, pp. 9843–9847, Dec. 1990.

[15] M. R. Urist, "Bone: formation by autoinduction," *Science*, vol. 150, no. 3698, pp. 893–899, Nov. 1965.

[16] J. Massagué and F. Weis-Garcia, "Serine/threonine kinase receptors: mediators of transforming growth factor beta family signals," *Cancer Surv.*, vol. 27, pp. 41–64, 1996.

[17] A. J. Celeste, J. A. Iannazzi, R. C. Taylor, R. M. Hewick, V. Rosen, E. A. Wang, and J. M. Wozney, "Identification of transforming growth factor beta family members present in bone-inductive protein purified from bovine bone," *Proc. Natl. Acad. Sci. U.S.A.*, vol. 87, no. 24, pp. 9843–9847, Dec. 1990.

[18] E. Ozkaynak, D. C. Rueger, E. A. Drier, C. Corbett, R. J. Ridge, T. K. Sampath, and H. Oppermann, "OP-1 cDNA encodes an osteogenic protein in the TGF-beta family," *EMBO J.*, vol. 9, no. 7, pp. 2085–2093, Jul. 1990.

[19] E. Ozkaynak, P. N. Schnegelsberg, D. F. Jin, G. M. Clifford, F. D. Warren, E. A. Drier, and H. Oppermann, "Osteogenic protein-2. A new member of the transforming growth factor-beta superfamily expressed early in embryogenesis," *J. Biol. Chem.*, vol. 267, no. 35, pp. 25220–25227, Dec. 1992.

[20] K. Tsuji, K. Cox, A. Bandyopadhyay, B. D. Harfe, C. J. Tabin, and V. Rosen, "BMP4 is dispensable for skeletogenesis and fracture-healing in the limb," *J Bone Joint Surg Am*, vol. 90 Suppl 1, pp. 14–18, Feb. 2008.

[21] A. Daluiski, T. Engstrand, M. E. Bahamonde, L. W. Gamer, E. Agius, S. L. Stevenson, K. Cox, V. Rosen, and K. M. Lyons, "Bone morphogenetic protein-3 is a negative regulator of bone density," *Nat. Genet.*, vol. 27, no. 1, pp. 84–88, Jan. 2001.

[22] D. Chen, M. Zhao, and G. R. Mundy, "Bone morphogenetic proteins," *Growth Factors*, vol. 22, no. 4, pp. 233–241, Dec. 2004.

[23] J. M. Granjeiro, R. C. Oliveira, J. C. Bustos-Valenzuela, M. C. Sogayar, and R. Taga, "Bone morphogenetic proteins: from structure to clinical use," *Braz. J. Med. Biol. Res.*, vol. 38, no. 10, pp. 1463–1473, Oct. 2005.

[24] J. M. Wozney, V. Rosen, A. J. Celeste, L. M. Mitsock, M. J. Whitters, R. W. Kriz, R. M. Hewick, and E. A. Wang, "Novel regulators of bone formation: molecular clones and activities," *Science*, vol. 242, no. 4885, pp. 1528–1534, Dec. 1988.

[25] E. A. Wang, V. Rosen, J. S. D'Alessandro, M. Bauduy, P. Cordes, T. Harada, D. I. Israel, R. M. Hewick, K. M. Kerns, and P. LaPan, "Recombinant human bone morphogenetic protein induces bone formation," *Proc. Natl. Acad. Sci. U.S.A.*, vol. 87, no. 6, pp. 2220–2224, Mar. 1990.

[26] K. Miyazono, "TGF-beta signaling by Smad proteins," *Cytokine Growth Factor Rev.*, vol. 11, no. 1–2, pp. 15–22, Jun. 2000.

[27] M. Zhao, Z. Zhao, J.-T. Koh, T. Jin, and R. T. Franceschi, "Combinatorial gene therapy for bone regeneration: cooperative interactions between adenovirus vectors expressing bone morphogenetic proteins 2, 4, and 7," *J. Cell. Biochem.*, vol. 95, no. 1, pp. 1–16, May 2005.

[28] Y. Zheng, G. Wu, J. Zhao, L. Wang, P. Sun, and Z. Gu, "rhBMP2/7 heterodimer: an osteoblastogenesis inducer of not higher potency but lower effective concentration compared with rhBMP2 and rhBMP7 homodimers," *Tissue Eng Part A*, vol. 16, no. 3, pp. 879–887, Mar. 2010.

[29] H. Nishitoh, H. Ichijo, M. Kimura, T. Matsumoto, F. Makishima, A. Yamaguchi, H. Yamashita, S. Enomoto, and K. Miyazono, "Identification of type I and type II serine/threonine kinase receptors for growth/differentiation factor-5," *J. Biol. Chem.*, vol. 271, no. 35, pp. 21345–21352, Aug. 1996.

[30] P. ten Dijke, H. Yamashita, T. K. Sampath, A. H. Reddi, M. Estevez, D. L. Riddle, H. Ichijo, C. H. Heldin, and K. Miyazono, "Identification of type I receptors for osteogenic protein-1 and bone morphogenetic protein-4," *J. Biol. Chem.*, vol. 269, no. 25, pp. 16985–16988, Jun. 1994.

[31] H. Yamashita, P. ten Dijke, D. Huylebroeck, T. K. Sampath, M. Andries, J. C. Smith, C. H. Heldin, and K. Miyazono, "Osteogenic protein-1 binds to activin type II receptors and induces certain activin-like effects," *J. Cell Biol.*, vol. 130, no. 1, pp. 217–226, Jul. 1995.

[32] H. Aoki, M. Fujii, T. Imamura, K. Yagi, K. Takehara, M. Kato, and K. Miyazono, "Synergistic effects of different bone morphogenetic protein type I receptors on alkaline phosphatase induction," *J. Cell. Sci.*, vol. 114, no. Pt 8, pp. 1483–1489, Apr. 2001.

[33] W. Zhu, J. Kim, C. Cheng, B. A. Rawlins, O. Boachie-Adjei, R. G. Crystal, and C. Hidaka, "Noggin regulation of bone morphogenetic protein (BMP) 2/7 heterodimer activity in vitro," *Bone*, vol. 39, no. 1, pp. 61–71, Jul. 2006.

[34] J. T. Koh, Z. Zhao, Z. Wang, I. S. Lewis, P. H. Krebsbach, and R. T. Franceschi, "Combinatorial gene therapy with BMP2/7 enhances cranial bone regeneration," *J. Dent. Res.*, vol. 87, no. 9, pp. 845–849, Sep. 2008.

[35] J. C. Kiefer, "Back to basics: Sox genes," *Dev. Dyn.*, vol. 236, no. 8, pp. 2356–2366, Aug. 2007.

[36] H. Akiyama, J.-E. Kim, K. Nakashima, G. Balmes, N. Iwai, J. M. Deng, Z. Zhang, J. F. Martin, R. R. Behringer, T. Nakamura, and B. de Crombrugghe, "Osteo-chondroprogenitor cells are derived from Sox9 expressing precursors," *Proc. Natl. Acad. Sci. U.S.A.*, vol. 102, no. 41, pp. 14665–14670, Oct. 2005.

[37] B. de Crombrugghe, V. Lefebvre, R. R. Behringer, W. Bi, S. Murakami, and W. Huang, "Transcriptional mechanisms of chondrocyte differentiation," *Matrix Biol.*, vol. 19, no. 5, pp. 389–394, Sep. 2000.

[38] H. Akiyama, "[Transcriptional regulation in chondrogenesis by Sox9]," *Clin Calcium*, vol. 21, no. 6, pp. 845–851, Jun. 2011.

[39] T. M. Schroeder, E. D. Jensen, and J. J. Westendorf, "Runx2: a master organizer of gene transcription in developing and maturing osteoblasts," *Birth Defects Res. C Embryo Today*, vol. 75, no. 3, pp. 213–225, Sep. 2005.

[40] M. P. Yavropoulou and J. G. Yovos, "The role of the Wnt signaling pathway in osteoblast commitment and differentiation," *Hormones (Athens)*, vol. 6, no. 4, pp. 279–294, Dec. 2007.

[41] F. Otto, A. P. Thornell, T. Crompton, A. Denzel, K. C. Gilmour, I. R. Rosewell, G. W. Stamp, R. S. Beddington, S. Mundlos, B. R. Olsen, P. B. Selby, and M. J. Owen, "Cbfa1, a candidate gene for cleidocranial dysplasia syndrome, is essential for osteoblast differentiation and bone development," *Cell*, vol. 89, no. 5, pp. 765–771, May 1997.

[42] P. Ducy, R. Zhang, V. Geoffroy, A. L. Ridall, and G. Karsenty, "Osf2/Cbfa1: a transcriptional activator of osteoblast differentiation," *Cell*, vol. 89, no. 5, pp. 747–754, May 1997.

[43] V. Geoffroy, M. Kneissel, B. Fournier, A. Boyde, and P. Matthias, "High bone resorption in adult aging transgenic mice overexpressing cbfa1/runx2 in cells of the osteoblastic lineage," *Mol. Cell. Biol.*, vol. 22, no. 17, pp. 6222–6233, Sep. 2002.

[44] Y. W. Zhang, N. Yasui, K. Ito, G. Huang, M. Fujii, J. Hanai, H. Nogami, T. Ochi, K. Miyazono, and Y. Ito, "A RUNX2/PEBP2alpha A/CBFA1 mutation displaying impaired transactivation and Smad interaction in cleidocranial dysplasia," *Proc. Natl. Acad. Sci. U.S.A.*, vol. 97, no. 19, pp. 10549–10554, Sep. 2000.

[45] K. Nakashima, X. Zhou, G. Kunkel, Z. Zhang, J. M. Deng, R. R. Behringer, and B. de Crombrugghe, "The novel zinc finger-containing transcription factor osterix is required for osteoblast differentiation and bone formation," *Cell*, vol. 108, no. 1, pp. 17–29, Jan. 2002.

[46] K. Park, T. Tsugawa, H. Furutachi, Y. Kwak, L. V. Liu, S. D. Wong, Y. Yoda, Y. Kobayashi, M. Saito, M. Kurokuzu, M. Seto, M. Suzuki, and E. I. Solomon, "Nuclear Resonance Vibrational Spectroscopy and DFT study of Peroxo-Bridged Biferric Complexes: Structural Insight into Peroxo Intermediates of Binuclear Non-heme Iron Enzymes," *Angew. Chem. Int. Ed. Engl.*, vol. 52, no. 4, pp. 1294–1298, Jan. 2013.

[47] K. M. Sinha and X. Zhou, "Genetic and molecular control of Osterix in skeletal formation," *Journal of Cellular Biochemistry*, p. n/a–n/a, 2012.

[48] K. Nakashima, X. Zhou, G. Kunkel, Z. Zhang, J. M. Deng, R. R. Behringer, and B. de Crombrugghe, "The novel zinc finger-containing transcription factor osterix is required for osteoblast differentiation and bone formation," *Cell*, vol. 108, no. 1, pp. 17–29, Jan. 2002.

[49] V. Lefebvre and P. Smits, "Transcriptional control of chondrocyte fate and differentiation," *Birth Defects Res. C Embryo Today*, vol. 75, no. 3, pp. 200–212, Sep. 2005.

[50] X. Yang, K. Matsuda, P. Bialek, S. Jacquot, H. C. Masuoka, T. Schinke, L. Li, S. Brancorsini, P. Sassone-Corsi, T. M. Townes, A. Hanauer, and G. Karsenty, "ATF4 is a substrate of RSK2 and an essential regulator of osteoblast biology; implication for Coffin-Lowry Syndrome," *Cell*, vol. 117, no. 3, pp. 387–398, Apr. 2004.

[51] G. Karsenty, "Minireview: transcriptional control of osteoblast differentiation," *Endocrinology*, vol. 142, no. 7, pp. 2731–2733, Jul. 2001.

[52] K. Arvidson, B. M. Abdallah, L. A. Applegate, N. Baldini, E. Cenni, E. Gomez-Barrena, D. Granchi, M. Kassem, Y. T. Konttinen, K. Mustafa, D. P. Pioletti, T. Sillat, and A. Finne-Wistrand, "Bone regeneration and stem cells," *Journal of Cellular and Molecular Medicine*, vol. 15, no. 4, pp. 718–746, Apr. 2011.

[53] L. Chang and M. Karin, "Mammalian MAP kinase signalling cascades," *Nature*, vol. 410, no. 6824, pp. 37–40, Mar. 2001.

[54] G. Mbalaviele, S. Sheikh, J. P. Stains, V. S. Salazar, S.-L. Cheng, D. Chen, and R. Civitelli, "Beta-catenin and BMP-2 synergize to promote osteoblast differentiation and new bone formation," *J. Cell. Biochem.*, vol. 94, no. 2, pp. 403–418, Feb. 2005.

[55] G. Rawadi, B. Vayssière, F. Dunn, R. Baron, and S. Roman-Roman, "BMP-2 controls alkaline phosphatase expression and osteoblast mineralization by a Wnt autocrine loop," *J. Bone Miner. Res.*, vol. 18, no. 10, pp. 1842–1853, Oct. 2003.

[56] B. H. Anderton, "Alzheimer's disease: clues from flies and worms," *Curr. Biol.*, vol. 9, no. 3, pp. R106–109, Feb. 1999.

[57] P. Polakis, "Wnt signaling and cancer," *Genes Dev.*, vol. 14, no. 15, pp. 1837–1851, Aug. 2000.

[58] F. Macian, "NFAT proteins: key regulators of T-cell development and function," *Nat. Rev. Immunol.*, vol. 5, no. 6, pp. 472–484, Jun. 2005.

[59] M. Wan and X. Cao, "BMP signaling in skeletal development," *Biochemical and Biophysical Research Communications*, vol. 328, no. 3, pp. 651–657, Mar. 2005.

[60] P. Kloen, D. Lauzier, and R. C. Hamdy, "Co-expression of BMPs and BMP-inhibitors in human fractures and non-unions," *Bone*, vol. 51, no. 1, pp. 59–68, Jul. 2012.

[61] R. Dimitriou, E. Jones, D. McGonagle, and P. V. Giannoudis, "Bone regeneration: current concepts and future directions," *BMC Med*, vol. 9, p. 66, 2011.

[62] J. W. Haycock, "3D Cell Culture: A Review of Current Approaches and Techniques," in *3D Cell Culture*, vol. 695, J. W. Haycock, Ed. Totowa, NJ: Humana Press, 2011, pp. 1–15.

[63] N. Laurens, P. Koolwijk, and M. P. M. de Maat, "Fibrin structure and wound healing," *J. Thromb. Haemost.*, vol. 4, no. 5, pp. 932–939, May 2006.

[64] P. Lei, R. M. Padmashali, and S. T. Andreadis, "Cell-controlled and spatially arrayed gene delivery from fibrin hydrogels," *Biomaterials*, vol. 30, no. 22, pp. 3790–3799, Aug. 2009.

[65] T.-W. Chung, M.-C. Yang, and W.-J. Tsai, "A fibrin encapsulated liposomes-in-chitosan matrix (FLCM) for delivering water-soluble drugs. Influences of the surface properties of liposomes and the crosslinked fibrin network," *Int J Pharm*, vol. 311, no. 1–2, pp. 122–129, Mar. 2006.

[66] M. W. Mosesson, K. R. Siebenlist, and D. A. Meh, "The structure and biological features of fibrinogen and fibrin," *Ann. N. Y. Acad. Sci.*, vol. 936, pp. 11–30, 2001.

[67] M. W. Mosesson, "Fibrinogen and fibrin structure and functions," *J. Thromb. Haemost.*, vol. 3, no. 8, pp. 1894–1904, Aug. 2005.

[68] H. Orbay, M. Tobita, and H. Mizuno, "Mesenchymal Stem Cells Isolated from Adipose and Other Tissues: Basic Biological Properties and Clinical Applications," *Stem Cells International*, vol. 2012, pp. 1–9, 2012.

[69] W. Wagner and A. D. Ho, "Mesenchymal Stem Cell Preparations—Comparing Apples and Oranges," *Stem Cell Reviews*, vol. 3, no. 4, pp. 239–248, Sep. 2007.

[70] P. Bourin, B. A. Bunnell, L. Casteilla, M. Dominici, A. J. Katz, K. L. March, H. Redl, J. P. Rubin, K. Yoshimura, and J. M. Gimble, "Stromal cells from the adipose tissue-derived stromal vascular fraction and culture expanded adipose tissue-derived stromal/stem cells: a joint statement of the International Federation for Adipose Therapeutics (IFATS) and Science and the International Society for Cellular Therapy (ISCT)," *Cytotherapy*, Apr. 2013.

[71] N. Cobb, G. Maxwell, and P. Silverstein, "The relationship of patient stress to burn injury," *J Burn Care Rehabil*, vol. 12, no. 4, pp. 334–338, Aug. 1991.

[72] C. Fehrer and G. Lepperdinger, "Mesenchymal stem cell aging," *Experimental Gerontology*, vol. 40, no. 12, pp. 926–930, Dec. 2005.

[73] C. Evans, "Gene therapy for the regeneration of bone," *Injury*, vol. 42, no. 6, pp. 599–604, Jun. 2011.

[74] W. Michlits, R. Mittermayr, R. Schäfer, H. Redl, and S. Aharinejad, "Fibrin-embedded administration of VEGF plasmid enhances skin flap survival," *Wound Repair Regen*, vol. 15, no. 3, pp. 360–367, Jun. 2007.

[75] M. Thomas and A. M. Klibanov, "Non-viral gene therapy: polycation-mediated DNA delivery," *Applied Microbiology and Biotechnology*, vol. 62, no. 1, pp. 27–34, Jul. 2003.

[76] X. Gao and L. Huang, "Cationic liposome-mediated gene transfer," *Gene Ther.*, vol. 2, no. 10, pp. 710–722, Dec. 1995.

[77] B. Ma, S. Zhang, H. Jiang, B. Zhao, and H. Lv, "Lipoplex morphologies and their influences on transfection efficiency in gene delivery," *J Control Release*, vol. 123, no. 3, pp. 184–194, Nov. 2007.

[78] M. Kanatani, T. Sugimoto, H. Kaji, T. Kobayashi, K. Nishiyama, M. Fukase, M. Kumegawa, and K. Chihara, "Stimulatory effect of bone morphogenetic protein-2 on osteoclast-like cell formation and bone-resorbing activity," *J. Bone Miner. Res.*, vol. 10, no. 11, pp. 1681–1690, Nov. 1995.

[79] H. Peng, V. Wright, A. Usas, B. Gearhart, H.-C. Shen, J. Cummins, and J. Huard, "Synergistic enhancement of bone formation and healing by stem cell-expressed VEGF and bone morphogenetic protein-4," *J. Clin. Invest.*, vol. 110, no. 6, pp. 751–759, Sep. 2002.

[80] W. Zhu, B. A. Rawlins, O. Boachie-Adjei, E. R. Myers, J. Arimizu, E. Choi, J. R. Lieberman, R. G. Crystal, and C. Hidaka, "Combined bone morphogenetic protein-2 and -7 gene transfer enhances osteoblastic differentiation and spine fusion in a rodent model," *J. Bone Miner. Res.*, vol. 19, no. 12, pp. 2021–2032, Dec. 2004.

[81] Y.-C. Huang, D. Kaigler, K. G. Rice, P. H. Krebsbach, and D. J. Mooney, "Combined angiogenic and osteogenic factor delivery enhances bone marrow stromal cell-driven bone regeneration," *J. Bone Miner. Res.*, vol. 20, no. 5, pp. 848–857, May 2005.

[82] Z. Zhao, M. Zhao, G. Xiao, and R. T. Franceschi, "Gene transfer of the Runx2 transcription factor enhances osteogenic activity of bone marrow stromal cells in vitro and in vivo," *Mol. Ther.*, vol. 12, no. 2, pp. 247–253, Aug. 2005.

[83] B. Levi, E. R. Nelson, K. Brown, A. W. James, D. Xu, R. Dunlevie, J. C. Wu, M. Lee, B. Wu, G. W. Commons, D. Vistnes, and M. T. Longaker, "Differences in osteogenic differentiation of adipose-derived stromal cells from murine, canine, and human sources in vitro and in vivo," *Plast. Reconstr. Surg.*, vol. 128, no. 2, pp. 373–386, Aug. 2011.

[84] A. Wang, X. Ding, S. Sheng, and Z. Yao, "Retinoic acid inhibits osteogenic differentiation of rat bone marrow stromal cells," *Biochem. Biophys. Res. Commun.*, vol. 375, no. 3, pp. 435–439, Oct. 2008.

[85] P. A. Zuk, M. Zhu, H. Mizuno, J. Huang, J. W. Futrell, A. J. Katz, P. Benhaim, H. P. Lorenz, and M. H. Hedrick, "Multilineage cells from human adipose tissue: implications for cell-based therapies," *Tissue Eng.*, vol. 7, no. 2, pp. 211–228, Apr. 2001.

[86] A. Wang, X. Ding, S. Sheng, and Z. Yao, "Bone morphogenetic protein receptor in the osteogenic differentiation of rat bone marrow stromal cells," *Yonsei Med. J.*, vol. 51, no. 5, pp. 740–745, Sep. 2010.

[87] J. E. Phillips, C. A. Gersbach, A. M. Wojtowicz, and A. J. García, "Glucocorticoid-induced osteogenesis is negatively regulated by Runx2/Cbfa1 serine phosphorylation," *J. Cell. Sci.*, vol. 119, no. Pt 3, pp. 581–591, Feb. 2006.

[88] L. Zeng, A. Worseg, G. Albrecht, W. Ohlinger, H. Redl, W. Grisold, K. Zatloukal, and G. Schlag, "Bridging of peripheral nerve defects with exogenous laminin-fibrin matrix in silicone tubes in a rat model," *Restor. Neurol. Neurosci.*, vol. 8, no. 3, pp. 107–111, Jan. 1995.

[89] M. Mana, M. Cole, S. Cox, and B. Tawil, "Human U937 monocyte behavior and protein expression on various formulations of three-dimensional fibrin clots," *Wound Repair Regen*, vol. 14, no. 1, pp. 72–80, Feb. 2006.

[90] P. Sun, J. Wang, Y. Zheng, Y. Fan, and Z. Gu, "BMP2/7 heterodimer is a stronger inducer of bone regeneration in peri-implant bone defects model than BMP2 or BMP7 homodimer," *Dental Materials Journal*, vol. 31, no. 2, pp. 239–248, 2012.

[91] N. S. Stott, T. X. Jiang, and C. M. Chuong, "Successive formative stages of precartilaginous mesenchymal condensations in vitro: modulation of cell adhesion by Wnt-7A and BMP-2," *J. Cell. Physiol.*, vol. 180, no. 3, pp. 314–324, Sep. 1999.

[92] A. Santos, A. D. Bakker, J. M. A. de Blieck-Hogervorst, and J. Klein-Nulend, "WNT5A induces osteogenic differentiation of human adipose stem cells via rho-associated kinase ROCK," *Cytotherapy*, vol. 12, no. 7, pp. 924–932, Nov. 2010.

8 Appendix

<u>Seqence of Wnt5a human mRNA (NM_003392.4)</u>

Highlighted sequences (pink and red) indicate splice variants of mRNA sequence of Wnt5a.

ACTAACTCGCGGCTGCAGGATCAGCGTCTGGAAGCAGACGTTTCGGCTACAGA
CCCAGAGAGGAGGAGCTGGAGATCAGGAGGCGTGAGCCGCCAAGAGTTTGCA
GAATCTGTGGTGTGAATGAACTGGGGGCACCTGGGCGCACAGATCGCCCCCCT
TCCCCCGCCCCGGGCCACAGTTGAGTAGTGGTACATTTTTTTCACCCTCTTGTG
AAGAATTTCTTTTTATTATTATTTGTCGTAAGGTCTTTTGCACAATCACGCCCACA
TTTGGGGTTGGAAAGCCCTAATTACCGCCGTCGCTGATGGACGTTGGAAACGG
AGCGCCTCTCCGTGGAACAGTTGCCTGCGCGCCCTCGCCGGACCGGCGGCTC
CCTAGTTGCGCCCCGACCAGGCCCTGCCCTTGCTGCCGGCTCGCGCGCGTCC
GCGCCCCCTCCATTCCTGGGCGCATCCCAGCTCTGCCCCAACTCGGGAGTCCA
GGCCCGGGCGCCAGTGCCCGCTTCAGCTCCGGTTCACTGCGCCCGCCGGACG
CGCGCCGGAGGACTCCGCAGCCCTGCTCCTGACCGTCCCCCCAGGCTTAACC
CGGTCGCTCCGCTCGGATTCCTCGGCTGCGCTCGCTCGGGTGGCGACTTCCTC
CCCGCGCCCCCTCCCCCTCGCCATGAAGAAGTCCATTGGAATATTAAGCCCAG
GAGTTGCTTTGGGGATGGCTGGAAGTGCAATGTCTTCCAAGTTCTTCCTAGTGG
CTTTGGCCATATTTTTCTCCTTCGCCCAGGTTGTAATTGAAGCCAATTCTTGGTG
GTCGCTAGGTATGAATAACCCTGTTCAGATGTCAGAAGTATATATTATAGGAGCA
CAGCCTCTCTGCAGCCAACTGGCAGGACTTTCTCAAGGACAGAAGAAACTGTGC
CACTTGTATCAGGACCACATGCAGTACATCGGAGAAGGCGCGAAGACAGGCAT
CAAAGAATGCCAGTATCAATTCCGACATCGAAGGTGGAACTGCAGCACTGTGGA
TAACACCTCTGTTTTTGGCAGGGTGATGCAGATAGGCAGCCGCGAGACGGCCT
TCACATACGCGGTGAGCGCAGCAGGGGTGGTGAACGCCATGAGCCGGGCGTG
CCGCGAGGGCGAGCTGTCCACCTGCGGCTGCAGCCGCGCCGCGCGCCCCAA
GGACCTGCCGCGGGACTGGCTCTGGGGCGGCTGCGGCGACAACATCGACTAT
GGCTACCGCTTTGCCAAGGAGTTCGTGGACGCCCGCGAGCGGGAGCGCATCC
ACGCCAAGGGCTCCTACGAGAGTGCTCGCATCCTCATGAACCTGCACAACAAC
GAGGCCGGCCGCAGGACGGTGTACAACCTGGCTGATGTGGCCTGCAAGTGCC
ATGGGGTGTCCGGCTCATGTAGCCTGAAGACATGCTGGCTGCAGCTGGCAGAC
TTCCGCAAGGTGGGTGATGCCCTGAAGGAGAAGTACGACAGCGCGGCGGCCA

TGCGGCTCAACAGCCGGGGCAAGTTGGTACAGGTCAACAGCCGCTTCAACTCG
CCCACCACACAAGACCTGGTCTACATCGACCCCAGCCCTGACTACTGCGTGCG
CAATGAGAGCACCGGCTCGCTGGGCACGCAGGGCCGCCTGTGCAACAAGACG
TCGGAGGGCATGGATGGCTGCGAGCTCATGTGCTGCGGCCGTGGCTACGACC
AGTTCAAGACCGTGCAGACGGAGCGCTGCCACTGCAAGTTCCACTGGTGCTGC
TACGTCAAGTGCAAGAAGTGCACGGAGATCGTGGACCAGTTTGTGTGCAAGTA
GTGGGTGCCACCCAGCACTCAGCCCCGCTCCCAGGACCCGCTTATTTATAGAA
AGTACAGTGATTCTGGTTTTTGGTTTTTAGAAATATTTTTTATTTTTCCCCAAGAAT
TGCAACCGGAACCATTTTTTTTCCTGTTACCATCTAAGAACTCTGTGGTTTATTAT
TAATATTATAATTATTATTTGGCAATAATGGGGGTGGGAACCAAGAAAAATATTTA
TTTTGTGGATCTTTGAAAAGGTAATACAAGACTTCTTTTGATAGTATAGAATGAAG
GGGAAATAACACATACCCTAACTTAGCTGTGTGGACATGGTACACATCCAGAAG
GTAAAGAAATACATTTTCTTTTTCTCAAATATGCCATCATATGGGATGGGTAGGTT
CCAGTTGAAAGAGGGTGGTAGAAATCTATTCACAATTCAGCTTCTATGACCAAAA
TGAGTTGTAAATTCTCTGGTGCAAGATAAAAGGTCTTGGGAAAACAAAACAAAAC
AAAACAAACCTCCCTTCCCCAGCAGGGCTGCTAGCTTGCTTTCTGCATTTTCAAA
ATGATAATTTACAATGGAAGGACAAGAATGTCATATTCTCAAGGAAAAAGGTAT
ATCACATGTCTCATTCTCCTCAAATATTCCATTTGCAGACAGACCGTCATATTCTA
ATAGCTCATGAAATTTGGGCAGCAGGGAGGAAAGTCCCCAGAAATTAAAAAATT
TAAAACTCTTATGTCAAGATGTTGATTTGAAGCTGTTATAAGAATTAGGATTCCAG
ATTGTAAAAAGATCCCCAAATGATTCTGGACACTAGATTTTTTTGTTTGGGGAGG
TTGGCTTGAACATAAATGAAAATATCCTGTTATTTTCTTAGGGATACTTGGTTAGT
AAATTATAATAGTAAAAATAATACATGAATCCCATTCACAGGTTCTCAGCCCAAG
CAACAAGGTAATTGCGTGCCATTCAGCACTGCACCAGAGCAGACAACCTATTTG
AGGAAAAACAGTGAAATCCACCTTCCTCTTCACACTGAGCCCTCTCTGATTCCTC
CGTGTTGTGATGTGATGCTGGCCACGTTTCCAAACGGCAGCTCCACTGGGTCC
CCTTTGGTTGTAGGACAGGAAATGAAACATTAGGAGCTCTGCTTGGAAAACAGT
TCACTACTTAGGGATTTTTGTTTCCTAAAACTTTTATTTTGAGGAGCAGTAGTTTT
CTATGTTTTAATGACAGAACTTGGCTAATGGAATTCACAGAGGTGTTGCAGCGTA
TCACTGTTATGATCCTGTGTTTAGATTATCCACTCATGCTTCTCCTATTGTACTGC
AGGTGTACCTTAAAACTGTTCCCAGTGTACTTGAACAGTTGCATTTATAAGGGGG
GAAATGTGGTTTAATGGTGCCTGATATCTCAAAGTCTTTTGTACATAACATATATA
TATATATACATATATATAAATATAAATATAAATATATCTCATTGCAGCCAGTGATTT
AGATTTACAGTTTACTCTGGGGGTTATTTCTCTGTCTAGAGCATTGTTGTCCTTCA

CTGCAGTCCAGTTGGGATTATTCCAAAAGTTTTTTGAGTCTTGAGCTTGGGCTGT
GGCCCTGCTGTGATCATACCTTGAGCACGACGAAGCAACCTTGTTTCTGAGGAA
GCTTGAGTTCTGACTCACTGAAATGCGTGTTGGGTTGAAGATATCTTTTTTCTTT
TCTGCCTCACCCCTTTGTCTCCAACCTCCATTTCTGTTCACTTTGTGGAGAGGGC
ATTACTTGTTCGTTATAGACATGGACGTTAAGAGATATTCAAAACTCAGAAGCAT
CAGCAATGTTTCTCTTTTCTTAGTTCATTCTGCAGAATGGAAACCCATGCCTATTA
GAAATGACAGTACTTATTAATTGAGTCCCTAAGGAATATTCAGCCCACTACATAG
ATAGCTTTTTTTTTTTTTTTTTAATAAGGACACCTCTTTCCAAACAGTGCCATCAA
ATATGTTCTTATCTCAGACTTACGTTGTTTTAAAAGTTTGGAAAGATACACATCTT
TCATACCCCCCTTAGGCAGGTTGGCTTTCATATCACCTCAGCCAACTGTGGCTC
TTAATTTATTGCATAATGATATTCACATCCCCTCAGTTGCAGTGAATTGTGAGCAA
AAGATCTTGAAAGCAAAAGCACTAATTAGTTTAAAATGTCACTTTTTTGGTTTTT
ATTATACAAAAACCATGAAGTACTTTTTTTATTTGCTAAATCAGATTGTTCCTTTTT
AGTGACTCATGTTTATGAAGAGAGTTGAGTTTAACAATCCTAGCTTTTAAAAGAA
ACTATTTAATGTAAAATATTCTACATGTCATTCAGATATTATGTATATCTTCTAGCC
TTTATTCTGTACTTTTAATGTACATATTTCTGTCTTGCGTGATTTGTATATTTCACT
GGTTTAAAAAACAAACATCGAAAGGCTTATGCCAAATGGAAGATAGAATATAAAA
TAAAACGTTACTTGTATATTGGTAAGTGGTTTCAATTGTCCTTCAGATAATTCATG
TGGAGATTTTTGGAGAAACCATGACGGATAGTTTAGGATGACTACATGTCAAAGT
AATAAAAGAGTGGTGAATTTTACCAAAACCAAGCTATTTGGAAGCTTCAAAAGGT
TTCTATATGTAATGGAACAAAAGGGGAATTCTCTTTTCCTATATATGTTCCTTACA
AAAAAAAAAAAAAAAGAAATCAAGCAGATGGCTTAAAGCTGGTTATAGGATTGCT
CACATTCTTTTAGCATTATGCATGTAACTTAATTGTTTTAGAGCGTGTTGCTGTTG
TAACATCCCAGAGAAGAATGAAAAGGCACATGCTTTTATCCGTGACCAGATTTTT
AGTCCAAAAAAATGTATTTTTTTGTGTGTTTACCACTGCAACTATTGCACCTCTCT
ATTTGAATTTACTGTGGACCATGTGTGGTGTCTCTATGCCCTTTGAAAGCAGTTT
TTATAAAAGAAAGCCCGGGTCTGCAGAGAATGAAAACTGGTTGGAAACTAAAG
GTTCATTGTGTTAAGTGCAATTAATACAAGTTATTGTGCTTTTCAAAAATGTACAC
GGAAATCTGGACAGTGCTCCACAGATTGATACATTAGCCTTTGCTTTTTCTCTTT
CCGGATAACCTTGTAACATATTGAAACCTTTTAAGGATGCCAAGAATGCATTATT
CCACAAAAAAACAGCAGACCAACATATAGAGTGTTTAAAATAGCATTTCTGGGCA
AATTCAAACTCTTGTGGTTCTAGGACTCACATCTGTTTCAGTTTTTCCTCAGTTGT
ATATTGACCAGTGTTCTTTATTGCAAAAACATATACCCGATTTAGCAGTGTCAGC
GTATTTTTTCTTCTCATCCTGGAGCGTATTCAAGATCTTCCCAATACAAGAAAATT

AATAAAAAATTTATATATAGGCAGCAGCAAAAGAGCCATGTTCAAAATAGTCATT
ATGGGCTCAAATAGAAGAAGACTTTTAAGTTTTAATCCAGTTTATCTGTTGAGTT
CTGTGAGCTACTGACCTCCTGAGACTGGCACTGTGTAAGTTTTAGTTGCCTACC
CTAGCTCTTTTCTCGTACAATTTTGCCAATACCAAGTTTCAATTTGTTTTTACAAA
ACATTATTCAAGCCACTAGAATTATCAAATATGACGCTATAGCAGAGTAAATACT
CTGAATAAGAGACCGGTACTAGCTAACTCCAAGAGATCGTTAGCAGCATCAGTC
CACAAACACTTAGTGGCCCACAATATATAGAGAGATAGAAAAGGTAGTTATAACT
TGAAGCATGTATTTAATGCAAATAGGCACGAAGGCACAGGTCTAAAATACTACAT
TGTCACTGTAAGCTATACTTTTAAAATATTTATTTTTTTTAAAGTATTTTCTAGTCT
TTTCTCTCTGTGGAATGGTGAAAGAGAGATGCCGTGTTTTGAAAGTAAGATGA
TGAAATGAATTTTTAATTCAAGAAACATTCAGAAACATAGGAATTAAAACTTAGAG
AAATGATCTAATTTCCCTGTTCACACAAACTTTACACTTTAATCTGATGATTGGAT
ATTTTATTTTAGTGAAACATCATCTTGTTAGCTAACTTTAAAAAATGGATGTAGAA
TGATTAAAGGTTGGTATGATTTTTTTTTAATGTATCAGTTTGAACCTAGAATATTG
AATTAAAATGCTGTCTCAGTATTTTAAAAGCAAAAAGGAATGGAGGAAAATTGC
ATCTTAGACCATTTTTATATGCAGTGTACAATTTGCTGGGCTAGAAATGAGATAA
AGATTATTTATTTTTGTTCATATCTTGTACTTTTCTATTAAAATCATTTTATGAAATC
CAAAAAAAAAAAAAAAAAAA

Sequence of Wnt 7a human mRNA (NM_004625.3)

Red sequence indicating Exon of mRNA of Wnt7a.

GAGGGGCGGGGGCTGGAGGCAGCAGCGCCCCCGCACTCCCCGCGTCTCGCA
CACTTGCACCGGTCGCTCGCGCGCAGCCCGGCGTCGCCCCACGCCGCGCTCG
CTCCTCCCTCCCTCCTCCCGCTCCGTGGCTCCCGTGCTCCTGGCGAGGCTCAG
GCGCGGAGCGCGCGGACGGGCGCACCGACAGACGGCCCCGGGGACGCCTCG
GCTCGCGCCTCCCGGGCGGGCTATGTTGATTGCCCCGCCGGGGCCGGCCCGC
GGGATCAGCACAGCCCGGCCCGCGGCCCCGGCGGCCAATCGGGACTATGAAC
CGGAAAGCGCGGCGCTGCCTGGGCCACCTCTTTCTCAGCCTGGGCATGGTCTA
CCTCCGGATCGGTGGCTTCTCCTCAGTGGTAGCTCTGGGCGCAAGCATCATCT
GTAACAAGATCCCAGGCCTGGCTCCCAGACAGCGGGCGATCTGCCAGAGCCG
GCCCGACGCCATCATCGTCATAGGAGAAGGCTCACAAATGGGCCTGGACGAGT
GTCAGTTTCAGTTCCGCAATGGCCGCTGGAACTGCTCTGCACTGGGAGAGCGC

ACCGTCTTCGGGAAGGAGCTCAAAGTGGGGAGCCGGGAGGCTGCGTTCACCTA
CGCCATCATTGCCGCCGGCGTGGCCCACGCCATCACAGCTGCCTGTACCCAGG
GCAACCTGAGCGACTGTGGCTGCGACAAAGAGAAGCAAGGCCAGTACCACCGG
GACGAGGGCTGGAAGTGGGGTGGCTGCTCTGCCGACATCCGCTACGGCATCG
GCTTCGCCAAGGTCTTTGTGGATGCCCGGGAGATCAAGCAGAATGCCCGGACT
CTCATGAACTTGCACAACAACGAGGCAGGCCGAAAGATCCTGGAGGAGAACAT
GAAGCTGGAATGTAAGTGCCACGGCGTGTCAGGCTCGTGCACCACCAAGACGT
GCTGGACCACACTGCCACAGTTTCGGGAGCTGGGCTACGTGCTCAAGGACAAG
TACAACGAGGCCGTTCACGTGGAGCCTGTGCGTGCCAGCCGCAACAAGCGGC
CCACCTTCCTGAAGATCAAGAAGCCACTGTCGTACCGCAAGCCCATGGACACG
GACCTGGTGTACATCGAGAAGTCGCCCAACTACTGCGAGGAGGACCCGGTGAC
CGGCAGTGTGGGCACCCAGGGCCGCGCCTGCAACAAGACGGCTCCCCAGGCC
AGCGGCTGTGACCTCATGTGCTGTGGGCGTGGCTACAACACCCACCAGTACGC
CCGCGTGTGGCAGTGCAACTGTAAGTTCCACTGGTGCTGCTATGTCAAGTGCAA
CACGTGCAGCGAGCGCACGGAGATGTACACGTGCAAGTGAGCCCCGTGTGCA
CACCACCCTCCCGCTGCAAGTCAGATTGCTGGGAGGACTGGACCGTTTCCAAG
CTGCGGGCTCCCTGGCAGGATGCTGAGCTTGTCTTTTCTGCTGAGGAGGGTAC
TTTTCCTGGGTTTCCTGCAGGCATCCGTGGGGGAAAAAAAATCTCTCAGAGCCC
TCAACTATTCTGTTCCACACCCAATGCTGCTCCACCCTCCCCCAGACACAGCCC
AGGTCCCTCCGCGGCTGGAGCGAAGCCTTCTGCAGCAGGAACTCTGGACCCCT
GGGCCTCATCACAGCAATATTTAACAATTTATTCTGATAAAAATAATATTAATTTA
TTTAATTAAAAAGAATTCTTCCACAAAAAAAAAAAAAAAAAA

9 Curriculum vitae

ALICE ZIMMERMANN
Franz-Mika-Weg 1a/1/14
1100 Wien
Tel.: (+43) 664 245 18 98
E-Mail: alicezimmermann@gmx.at

PERSÖNLICHE INFORMATIONEN

- Geburtsdatum: 15.06.1989
- Geburtsort: Wien
- Geburtsland: Österreich
- Religionsbekenntnis: röm.-kath.
- Staatsbürgerschaft: Österreich

SCHULBILDUNG

- September 1995 – Juni 1999
  Volkschule des Institutes Neulandschulen 1100 Wien
  Ludwig von Höhnel Gasse 17-19
- September 1999 – Juni 2007
  Gymnasium des Institutes Neulandschulen 1100 Wien
  Ludwig von Höhnel Gasse 17-19
- Juni 2007 Schulabschluss mit Matura

HOCHSCHULBILDUNG

- Oktober 2007 – Mai 2011
  Bachelorstudium Biologie an der Hauptuniversität Wien
  Schwerpunkt: Mikrobiologie/Genetik
- Mai 2011 – heute
  Masterstudiums Molekulare Biologie
  Schwerpunkt: Molekulare Medizin
- Oktober 2013 – heute
  Medizinstudium an der Medizinischen Universität Wien

SPRACHKENNTNISSE

- Muttersprache: Deutsch
- Fremdsprachen: Englisch, Französisch

BERUFSSERFAHRUNGEN

- August 2007 – Februar 2013
  Molekularbiologische Mitarbeiterin im Ludwig Boltzmann Institut für Experimentelle und Klinische Traumatologie
- Februar 2012 – Juli 2012
  Wahlbeispiel „Molekulare Medizin" zumThema „Non-viral gene delivery with agarose hydrogel based gene activated matrices (GAMs) for osteochondral interface tissue engineering"
- März 2012 - Juli 2013
  Masterarbeit im Ludwig Boltzmann Institut für Experimentelle und Klinische Traumatologie
- September 2012
  Mitarbeit beim TERMIS World Congress 2012 "Tissue Engineering and Regenerative Medicine"

PUBLIKATIONEN

- Enhanced reporter gene assay for the detection of osteogenic differentiation. Feichtinger GA, Morton TJ, **Zimmermann A**, Dopler D, Banerjee A, Redl H, van Griensven M.

- Inducible and constitutive co-expression systems for non-viral osteoinductive gene therapy. G. A. Feichtinger, A.T.Hoffmann, K. Wassermann, **A. Zimmermann**, M.van Griensven, H. Redl

ZUSATZQUALIFIKATIONEN

- EDV: MS Office
- Führerschein (Klasse B)
- Absolvierte Kurse:
  - Erste Hilfe Schulung

HOBBIES

- Volleyball
- Skifahren
- Malen
- Reisen

Alice Zimmermann